The Journal of Neuroscience, January 15, 2001, 21(2):513–526

Abnormalities of Male-Specific FRU Protein and Serotonin Expression in the CNS of *fruitless* Mutants in *Drosophila*

Gyunghee Lee and Jeffrey C. Hall

Department of Biology, Brandeis University, Waltham, Massachusetts 02454

The *fruitless* gene in *Drosophila* produces male-specific protein (FRU^M) involved in the control of courtship. FRU^M spatial and temporal patterns were examined in *fru* mutants that exhibit aberrant male courtship. Chromosome breakpoints at the locus eliminated FRU^M. Homozygous viable mutants exhibited an intriguing array of defects. In fru^1 males, there were absences of FRU^M-expressing neuronal clusters or stained cells within certain clusters, reductions of signal intensities in others, and ectopic FRU^M expression in novel cells. fru^2 males exhibited an overall decrement of FRU^M expression in all neurons normally expressing the gene. fru^4 and fru^{sat} mutants only produced FRU^M in small numbers of neurons at extremely low levels, and no FRU^M signals were detected in fru^3 males. This array of abnormalities was inferred to correlate with the varying behavioral defects exhibited by these mutants. Such abnormalities include courtship among males, which has been hypothesized to involve anomalies of serotonin (5-HT) function in the brain. However, double-labeling uncovered no coexpression of FRU^M and 5-HT in brain neurons. Yet, a newly identified set of sexually dimorphic FRU^M/5-HT-positive neurons was identified in the abdominal ganglion of adult males. These sexually dimorphic neurons (s-Abg) project toward regions of the abdomen involved in male reproduction. The s-Abg neurons and the proximal extents of their axons were unstained or absent in wild-type females and exhibited subnormal or no 5-HT immunoreactivity in certain *fru*-mutant males, indicating that *fruitless* controls the formation of these cells or 5-HT production in them.

Key words: fruitless *transposons; chromosome aberrations; brain neurons; ventral nerve cord; sexual dimorphism; serotonergic neurons*

Courtship in *Drosophila melanogaster* is regulated by a somatic sex-determination hierarchy. One of the "downstream" genes functioning within this hierarchy is *fruitless* (for review, see Goodwin, 1999; Yamamoto and Nakano, 1999). *fru* mutations cause the most sharply defined effects on male courtship, compared with behaviorally mutant phenotypes associated with other downstream genes (Villella and Hall, 1996; Finley et al., 1997). *fruitless* produces male- and female-specific transcripts under the control of a distal promoter (P1) located ~100 kb from the bulk of the open reading frame of the gene (Ryner et al., 1996). The male-specific proteins (FRU^Ms) encoded by P1-controlled mRNAs are likely to be involved in the regulation of courtship or the development of the neural substrates for male reproductive behavior (Goodwin 1999). In females, P1-produced transcripts are not translated into detectable FRU protein (Lee et al., 2000; Usui-Aoki et al., 2000).

One approach toward understanding how *fru* regulates male courtship is to compare patterns of FRU^M expression in the CNS of various *fruitless* mutants that display behavioral phenotypes ranging from mildly to severely defective (Villella et al., 1997; Goodwin et al., 2000). The courtship subnormalities and bisexual behavior caused by *fru* mutations could be understood in terms of where FRU^M is expressed in the CNS (or not expressed, as the case may be) in a given mutant.

The fact that several *fru*-mutant types court other males might be attributable to subnormal levels of serotonin (5-HT) in relevant brain cells. This hypothesis suggested itself because of the anomalous inter-male courtships that are induced by ectopic expression of the *white* (w^+) gene (Zhang and Odenwald, 1995; Hing and Carlson, 1996). *white* encodes a tryptophan–guanine transporter; because tryptophan is a precursor of 5-HT, induced w^+ expression all over the brain could cause subnormal 5-HT levels in neurons that normally produce it. Drug-induced 5-HT reductions can induce homosexual behavior of male mammals (for review, see Gessa and Tagliamonte, 1974; Fratta et al., 1977). *fru* mutants, which are predicted to exhibit deficits in male-specific transcription factors encoded by this gene (Goodwin, 1999; Goodwin et al., 2000), could also be deficient in 5-HT if its production is downstream of FRU^M function. Moreover, the actions of both ectopic-w^+ and *fruitless* have been suggested to be in the same pathway because of a blockade of the behavioral effects of ectopic-w^+ by a *fru* mutation that, by itself, causes very low levels of male courtship (Nilsson et al., 2000). Based on these suppositions, we analyzed the relationship between the spatial distribution of 5-HT and *fru* gene products in normal and mutant CNSs.

Along with demonstrating that elements of 5-HT production are downstream of *fru* functioning (although not in CNS regions that one might have expected), this feature of the study provided the first information on axonal projections of certain FRU^M cells. Assessing the subcellular localization of FRU^M alone gives no insight into this matter; FRU immunoreactivities are nuclear (Lee et al., 2000), consistent with the supposition that these proteins are gene regulators.

Received May 18, 2000; revised Oct. 3, 2000; accepted Oct. 30, 2000.

This work was supported by National Institutes of Health (NIH) Grants NS-33352 and GM-21473, and NIH Neuroscience Training Grant 5T32-NS-07292. We thank Jae H. Park, Adriana Villella, Stephen F. Goodwin, Jean-Christophe Billeter, Bruce S. Baker, and Barbara J. Taylor for helpful discussions, and we appreciate comments on this manuscript from Barbara J. Taylor, Margit Foss, and Ralph J. Greenspan. We thank Edward Dougherty and Maki Kaneko for confocal and photographic assistance, and Barbara Beltz and Kalpana White for advice about anti-5-HT immunohistochemistry.

Correspondence should be addressed to Jeffrey C. Hall, Department of Biology, MS-008, Brandeis University, Waltham, MA 02454-9110. E-mail: hall@brandeis.edu.

Dr. Lee's present address: Department of Biochemistry and Cellular and Molecular Biology, University of Tennessee, Knoxville, TN 37996-0840.

MATERIALS AND METHODS

Strains and culturing. Stocks and progeny from crosses of *D. melanogaster* were reared in 12 hr light/dark (LD) cycles at 25°C, 70% relative humidity, on a sucrose–cornmeal–yeast medium containing the mold inhibitor Tegosept. A Canton-S strain was used as the wild-type control.

The *fruitless* mutant stocks fru^1, fru^2, fru^3, fru^4, and fru^{sat} were maintained as described in Villella et al. (1997) and Goodwin et al. (2000). The following homozygous-lethal *fru* variants, missing all or part of the locus, were combined in pairwise crosses (see Table 1): $Df(3R)Cha^{M5}$, *Df(3R)P14*, $Df(3R)fru^{sat15}$, $Df(3R)fru^{w24}$, and $Df(3R)fru^{4-40}$ (Gailey and Hall, 1989; Ito et al., 1996; Ryner et al., 1996; Anand et al., 2001). These deletions will be referred to as $Df\text{-}Cha^{M5}$, *Df-P14*, $Df\text{-}sat^{15}$, $Df\text{-}fru^{w24}$, and $Df\text{-}fru^{4-40}$. The lethal variants fru^{w12} and fru^{w27}, each carrying single breakpoints within the locus, were crossed to each other or to certain *Df*-bearing flies to generate severely lesioned genotypes (see Table 1). The *Df-fru* or *fru*-lethal stocks were balanced with *In(3LR)TM6B, Tb*, *In(3LR)TM3*, *Sb*, or *Tp(3)MKRS, Sb*.

To obtain 2-d-old pupae homozygous for a *fru* mutation or carrying a given transheterozygous combination, flies from *TM6B*-balanced stocks were crossed to each other. This was necessary because of the homozygous lethality or sterility associated with *fru* variants, with the exception of fru^2, which is homozygous-viable and fertile (permitting pupae to be obtained from a true-breeding stock). For the other strains, balancer-over-*fru* heterozygotes were crossed, and animals not expressing the pupal marker *Tb* were selected. To stage these developing animals, white prepupae were selected, sexed by gonadal size, and maintained on a Petri dish with a wet filter paper at 25°C, 70% relative humidity, on a 12 hr LD cycle for 2 d. To collect homozygous or transheterozygous *fru*-mutant adults, *TM3*- or *MKRS*-balanced *fru* stocks were used; progeny not expressing the *Sb* marker were selected.

Immunohistochemistry and in situ *hybridization.* Polyclonal anti-FRU^M, designed to detect male-specific proteins encoded by male-specific *fru* transcripts stemming from the action of the sex-specific P1 promoter, was generated in a rat as described in Lee et al. (2000). Anti-FRU^M-mediated staining was effected using whole-mounts of dissected CNSs from 2-d-old pupae and 4- to 7-d-old adults. The antibody was applied at a dilution of 1:300. To detect cell and tissue labeling mediated by such application, two different secondary antibodies were used. (1) Horseradish peroxidase-conjugated anti-rat serum (made in donkey; Jackson ImmunoResearch, West Grove, PA) was applied at a dilution of 1:200. For the color reaction, the tissues were incubated at room temperature in the dark for 20 min in phosphate buffer containing 0.5 mg/ml 3,3′-diaminobenzidine tetrahydrochloride; 0.0015% hydrogen peroxide solution was added, and the color development was monitored under a dissecting microscope. After sufficient color had developed, the reaction was terminated by rinsing tissues with distilled water. Stained tissues were rinsed three times in phosphate buffer, dehydrated, cleared in glycerol, and mounted in 100% glycerol under glass coverslips. (2) For fluorescent immunostaining, fluorescein isothiocyanate (FITC)-conjugated secondary IgG (made in donkey; Jackson ImmunoResearch) was used at a dilution of 1:200. CNSs labeled in this manner were mounted with 2% *n*-propyl gallate in 80% glycerol in phosphate buffer, pH 7.4. Preparations were observed under a Zeiss Axiophot microscope or an MRC600 laser-scanning confocal microscope (Bio-Rad, Richmond, CA).

To apply anti-5-HT (made in rabbit; Protos Biotech, New York, NY) for immunohistochemistry, CNSs were fixed in a solution of 4% paraformaldehyde including 7.5% picric acid for 1 hr at room temperature; this antibody was used at a dilution of 1:500. The secondary antisera, FITC-conjugated anti-rabbit IgG (made in donkey; Jackson ImmunoResearch), was used at a dilution of 1:200, applying the same procedures used for anti-FRU^M immuno-histochemistry.

Immunofluorescent double-labelings were performed on whole-mounted CNSs; anti-FRU^M (from rat) and anti-5-HT (from rabbit) were applied to whole-mounted CNSs of wild-type adult males. Dissection, fixation, and washes were performed as described above for anti-5-HT, except for the fixation, which was done on ice. FITC-conjugated anti-rat IgG for anti-FRU^M and lissamine rhodamine sulfonyl chloride-conjugated anti-rabbit IgG (from donkey; Jackson ImmunoResearch) for anti-5-HT were used as secondary antisera. Preparations were viewed in the confocal microscope described above, which is equipped with an argon–krypton laser and dual-channel scanning. Colocalization was verified by merging the two channels.

For *in situ* hybridization with whole-mounted CNSs, an antisense probe from the P1 region of the *fru* locus (see Fig. 1) was applied to CNSs dissected from 1-d-old $Df\text{-}fru^{4-40}/Df\text{-}sat^{15}$ or $Df\text{-}Cha^{M5}/Df\text{-}sat^{15}$ (double-deletion) male pupae. The particular probe (called P1.S1; see Fig. 1) and the labeling procedures were as described in Lee et al. (2000).

Scoring of staining intensities. To analyze the levels of FRU^M in CNSs of viable *fru* mutants and wild-type males, fluorescently immunostained signals from various FRU^M-expressing neuronal clusters in whole-mounted CNS were quantified as described in Lee et al. (2000). We focused on three such clusters within the superior protocerebrum in analyzing the wild type and the *fru* mutants. These and other FRU^M cell groups had staining intensities assessed for animals carrying the various *fru* genotypes (see Table 2 legend). The FRU^M immunostaining quantifications were performed on whole-mounted brains dissected from 2-d-old pupae, which show the highest level of CNS expression by this protein (Lee et al., 2000), and from 4- to 7-d-old adults, which are active courters. The specimens to be compared (in terms of genotype or life-cycle stage) were processed simultaneously to minimize signal variations that could occur for nonsubstantive reasons. At least five CNSs were sampled from animals of each genotype at both of the different stages. The dorsoanterior brain region that contains both neuronal clusters was imaged at 100× magnification by confocal microscopy (2 or 4 μm optical sections). Staining intensities for nuclei of cells within these two clusters were obtained (as pixel values) from at least five individual brains by applying an Adobe PhotoShop (3.0) tool called Histogram. This permitted an average value to be computed from several strongly stained nuclei in the cells of the two nearby clusters; for a given brain, such an average value was obtained for only the left or right hemisphere. The relevant FRU^M signal values ranged from black to white (of 256 gray values); "whitest" represents maximal protein expression (see Table 2 for additional details).

To assess levels of FRU^M expression in CNSs of 2-d-old pupae that carried transheterozygous *Df*s or were homozygous for the fru^3 mutation, protein expression was scored subjectively in whole-mounts (3–10 individual specimens for each genotype) using a fluorescent microscope at 40× magnification. A representative image for each genotype was obtained using confocal microscopy afterward. To assess staining intensities from CNSs subjected to P1-*fru*-probe *in situ* hybridization, at least six specimens were subjectively evaluated using brightfield microscopy. A representative image for an animal of a given *fru* genotype was obtained at 30× magnification.

5-HT uptake. In attempts to determine whether the lack of 5-HT immunostaining in the abdominal ganglion of the fru^3 mutant (see Results) is attributable to the absence of the relevant cells (those that contain signal in wild type) or a dearth of serotonin synthesis, ventral nerve cords (VNCs) of 4- to 5-d-old adult males were dissected and exposed to exogenously applied 5-HT, essentially as described in Vallés and White (1986). Tissues were incubated in *Drosophila* Ringer's [(in mM) 130 NaCl, 4.7 KCl, 1.8 $CaCl_2$, 0.74 KH_2PO_4, and 0.35 Na_2HPO_4] containing a 5-HT/creatine-sulfate (Sigma, St. Louis, MO) at the following concentrations: 1, 5, 10, 100, and 500 μM. The VNCs were rinsed three times for 15 min each in ice-cold Ca^{2+}-free Ringer's, then fixed with 4% paraformaldehyde with 7.5% picric acid for 1 hr at room temperature. Application of primary anti-5-HT and subsequent immunohistochemical procedures were as described above (see Immunohistochemistry and *in situ* hybridization).

RESULTS

Male-specific *fru* products in the CNS of chromosome-breakpoint variants

Among the most severely defective *fru* variants in terms of courtship behavioral subnormalities are those expressing the effects of chromosome breakpoints within the locus. We suspected that animals carrying most or all of these genotypes would lack detectable FRU^M. This expectation is based on the molecular characterization of these chromosome aberrations (Fig. 1) against a background of the *fru* transcript-types that are produced under the control of a given promoter (Ryner et al., 1996; Goodwin et al., 2000). In fact, two of the *fru* variants in question (Fig. 1) were shown to be null for FRU^M immunostaining: the $Df\text{-}Cha^{M5}/Df\text{-}P14$ and $Df\text{-}fru^{4-40}/Df\text{-}P14$ double-deletion types (Lee et al., 2000). These assessments were performed principally as a control for specificity of the antibody.

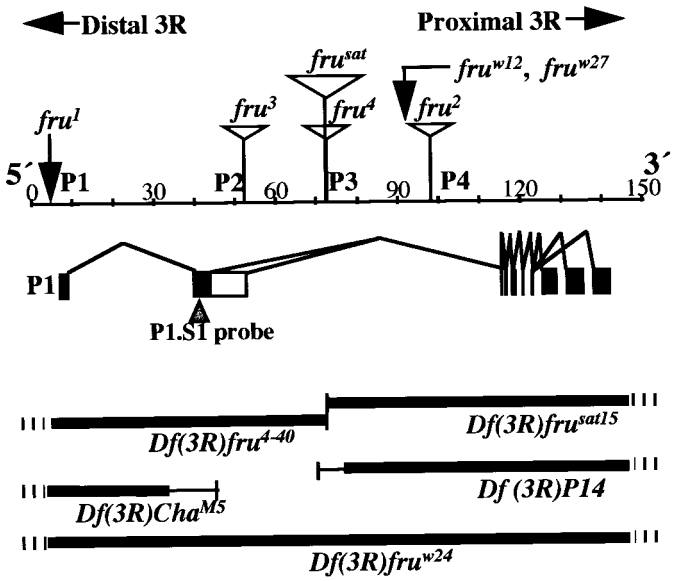

Figure 1. The *fruitless* gene and genetic variations at the locus. This large (~130 kb) gene contains at least four promoters (Ps); the 5′-most promoter (*P1*, *left*) controls the production of primary transcripts that are sex-specifically spliced with respect to the second exon (Ryner et al., 1996; Goodwin et al., 2000). P1-promoted RNA species are diagrammed in the *middle panel*. The principal alternative splicings of interest occur near the 5′ (*left*) end. (There are additional such splicings near the 3′ end, designated by three *black rectangles* on the *right* that result in different kinds of Zn-finger pairs near the C termini of FRU protein isoforms.) The 5′ sex-specific splicings result in a male mRNA of which relatively 5′ coding sequences (5′ ORF) are translated to produce 101 male-specific amino acids bound to the remainder of the residues that are encoded by relatively 3′ sequences emanating from the *right* part of the gene. This protein is called FRU^M, which is specifically detected by an antibody generated against the male-specific N-terminal residues (Lee et al., 2000). In females, the 5′ ORF runs into a stop codon after nucleotides encoding 94 amino acids (because of the alternative splicing referred to above). A ~280-nucleotide probe applied in this study to detect sex-specifically spliced transcripts (cf. Lee et al., 2000) corresponds to sequences in the second exon, designated by a *black rectangle* (*middle left*) and pointed to by an *inverted triangle*. Sex-nonspecific promoters (*P2*, *P3*, and *P4*) are used to generate transcripts that lack the male-specific 101 residues and are believed to be associated with vital *fru* functions that operate in both sexes (Ryner et al., 1996; Anand et al, 2001). Such functions are inferred (in part) from the effects of fru^{w12} and fru^{w27}, which are translocation and inversion breakpoints that cause late-developmental lethality when they are homozygous or heterozygous for a deletion that eliminates the entire locus. fru^{w24} is such a deletion (*Df*), indicated by the *thick black line* (this and other such lines designate deleted material); *hash marks* (for this and the other *Df*s) indicate that the deletion extends well beyond the locus. The four additional *Df*s that were applied have breakpoints within the locus (Ito et al., 1996; Ryner et al., 1996; Anand et al, 2001), as indicated by *thin vertical lines* (the *thin horizontal portions* of these *Df* indicators imply not-quite-certain breakpoint determinations). Homozygous-viable *fruitless* mutants are caused, in one case, by an inversion breakpoint (fru^1) and, in the remaining cases, by transposon inserts (*open triangles*) inserted at intragenic locations as determined by Ito et al. (1996), Ryner et al., (1996), and Goodwin et al. (2000). These and other features of the diagram are based on results in these three reports, as well as information obtained by interrogating the *Drosophila* genome database at www.fruitfly.org with sequences of various *fru* cDNAs (Lee et al., 2000) and molecular determination of the fru^1 inversion breakpoint, which was found to be 3.3 kb upstream (to the *left*) of the transcription start site for RNAs generated under the control of the P1 promoter. The beginning of a 7 bp consensus-sequence for the latter starts 28 bp downstream of the transcription start (T. Carlo, S. F. Goodwin, J.-C. Billeter, L. C. Ryner, B. S. Baker, and J. C. Hall, unpublished observations).

Drosophila carrying the $Df\text{-}Cha^{M5}/Df\text{-}P14$ or $Df\text{-}fru^{4-40}/Df\text{-}P14$ deletions develop into viable adults, as can be rationalized by their ability to transcribe *fru* mRNAs under the control of one or more promoters located downstream of P1 (Fig. 1). These transcripts encode FRU protein isoforms that are produced in both males and females (Lee et al., 2000); absence of these products, caused by radiation-induced *fru*-locus lesions (Ryner et al., 1996) associated with chromosomal breakpoints located between the P1 and P4 promoters (Fig. 1), leads to near lethality of males and females (Anand et al., 2001). The $Df\text{-}Cha^{M5}/Df\text{-}P14$ and $Df\text{-}fru^{4-40}/Df\text{-}P14$ combinations [in which P4 and possibly P3 are active, but P1 is deleted (Fig. 1)] allow for normal viability; males of these genotypes exhibit severely subnormal levels of courtship and do not mate (Villella et al., 1997; Anand et al., 2001).

Two further double-deletion types cause similar subnormalities of male courtship: $Df\text{-}Cha^{M5}/Df\text{-}sat^{15}$ and $Df\text{-}fru^{4-40}/Df\text{-}sat^{15}$, whose levels of courtship directed at females are nearly zero (Anand et al, 2001). As expected from the positions of the intra-*fru* breakpoints associated with these three deletions (Fig. 1), neither P1-promoted transcripts (Fig. 2*A*) nor FRU^M protein (Table 1) was detected in males of these two genotypes. Actually, it could be that a transcript fragment containing sequences from the 5′ end of P1-promoted mRNA would have been labeled by the probe applied (Fig. 1); and that the male-specific, N-terminal residues encoded by these 5′ sequences would be present as an anti-FRU^M-labeled oligopeptide (Fig. 1). That no signals were detected by the nucleic acid or the antibody probe (Fig. 2*A*; Table 1) indicates that the truncated forms of neither *fru* transcript nor FRU protein accumulate to levels detectable by *in situ* hybridization or immunohistochemistry. These results are consistent with previous results obtained from histological analyses of $Df\text{-}Cha^{M5}/Df\text{-}P14$ and $Df\text{-}fru^{4-40}/Df\text{-}P14$ males (Lee et al., 2000).

There is an additional category of intralocus lesions associated with the *fru* gene: inversion and translocation breakpoints called fru^{w12} and fru^{w27}. These are located between P1 and the 3′-*fru* ORF, relatively close to the latter (Ryner et al., 1996) (Fig. 1). When fru^{w27} or fru^{w12} is heterozygous with a deletion that removes relatively 5′ sequences ($Df\text{-}Cha^{M5}$ or $Df\text{-}fru^{4-40}$), the result is a viable adult that (as a male) exhibits almost no courtship (Ryner et al., 1996; Anand et al, 2001. When either of these proximally located breakpoints is heterozygous with a full *fru* deletion (Fig. 1, $Df\text{-}fru^{w24}$), or in a transheterozgote carrying the two lesions, the result is late developmental lethality (Ryner et al., 1996). All of these fru^{w27}- and fru^{w12}-including genotypes would be expected to eliminate FRU^M protein, provided that the aforementioned N-terminal oligopeptide cannot accumulate to detectable levels. These expectations were met (Fig. 2*B*; Table 1).

FRU^M in the CNS of homozygous-viable *fruitless* mutants

The other genetic variations involving the *fruitless* gene are homozygous viable mutants, most of which are caused by transposons inserted within the locus (Fig. 1). The transposons in the four relevant mutants (Ito et al., 1996; Ryner et al., 1996; Goodwin et al., 2000) are inserted between the P1 promoter and the bulk of the open reading frame of *fru* (Fig. 1). Thus, the P1 promoter itself should be active in these mutants. Indeed, *in situ* hybridizations using a sex-specific probe (like that applied in the current study) (Fig. 1) revealed signal patterns in these mutants similar to that of wild type (Goodwin et al., 2000). Therefore, transcriptional activity of the P1 promoter per se seems unim-

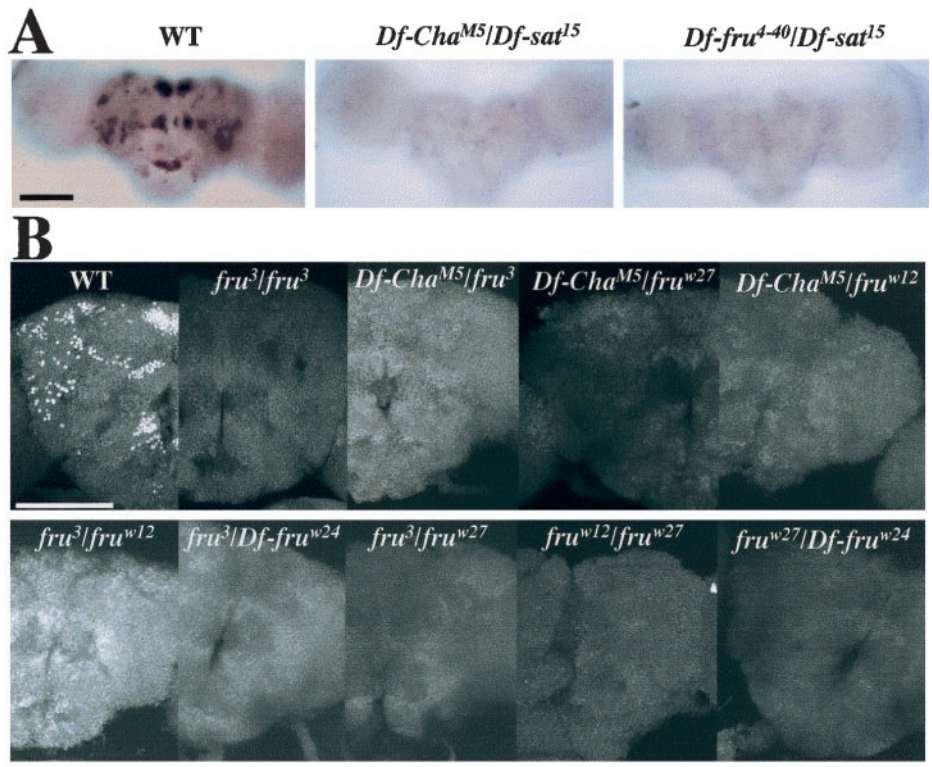

Figure 2. Lack of sex-specific *fruitless* expression in the CNS of *fru*-breakpoint mutants. *A*, *In situ* hybridizations performed on pupal progeny resulting from crosses involving three of the deletions depicted in Figure 1; 1-d-old male pupae had a *fru*-derived riboprobe (Fig. 1) applied to whole-mounted CNSs of wild type (WT, $n = 11$) and these two *Df*/*Df* types (*Df-Cha*^{M5}/*Df-sat*^{15}, $n = 6$; *Df-fru*$^{4-40}$/*Df-sat*^{15}, $n = 6$); no signals were elicited by this nucleic-acid probe in any of the 12 double-deletion specimens. *B*, Anti-FRU^M immunohistochemistry performed on pupal progeny resulting from crosses of various deletions and other breakpoint variants (Fig. 1); heterozygotes involving certain of the chromosome aberrations and one of the *fru* transposon mutants were included as a negative control (compare Fig. 3; Table 2); antibody against the male-specific form of the protein was applied to whole-mounted CNSs dissected from 2-d-old male pupae. Summaries of these immunohistochemical results (including numbers of samples per genotype) are given in Table 1. Signals (or the absence thereof) were examined by confocal microscopy, and representative images were made for specimens of the various genotypes at 40×. *A*, *B*, anterior views of the brains. *B*, The brain image of *fru*^{3}/*fru*^{w12} (*lower left panel*) shows a *whitish* general background staining that was not detected in other specimens of this genotype (cf. Table 1) and bears no relation to the WT pattern. Scale bars: *A*, 100 μm; *B*, 50 μm.

Table 1. Lack of male-specific FRU^M protein in severely affected *fruitless* mutants

Genotype	Relative FRU^M immunostaining, % (*n* pupal CNS specimens)
WT	100 (10)
fru^3/*fru*^{3}	0 (6)
fru^{w12}/*fru*^{3}	0 (3)
Df-fru^{w24}/*fru*^{3}	0 (5)
fru^{w27}/*fru*^{3}	0 (5)
fru^3/*Df-Cha*^{M5}	0 (7)
fru^{w12}/*Df-Cha*^{M5}	0 (7)
fru^{w27}/*Df-Cha*^{M5}	0 (5)
fru^{w12}/*Df-fru*^{w24}	0 (3)
fru^{w12}/*fru*^{w27}	0 (3)
Df-fru^{w24}/*fru*^{w27}	0 (3)
Df-Cha^{M5}/*Df-sat*^{15}	0 (5)
Df-fru$^{4-40}$/*Df-sat*^{15}	0 (5)

Immunohistochemistry using anti-FRU^M was performed to assess expression of the male forms of FRU protein in the CNSs of 2-d-old male pupae from a wild-type (WT) stock, a *fru*^{3}-bearing strain, and pupal progeny resulting from crosses of *fru*-breakpoint variants to each other or certain such variants to *fru*^{3} (the only homozygous-viable mutant used here). The *w*-including genotypes are chromosome aberrations, each involving a breakpoint within the *fru* locus; most of the *Df*-including genotypes are deletions, each of which has one breakpoint at this locus and thus is missing part of the locus (*Df-fru*^{w24} removes the entire locus). Nearly all breakpoint combinations, with respect to the chromosome aberrations depicted in Figure 1, were generated, except for *fru*^{w24}/*Df-Cha*^{M5} (which die as embryos). For the results column, the wild-type staining level was simply set at 100, because there was no apparent FRU^M immunostaining in pupae carrying any of these mutant or *fru*-breakpoint variant specimens.

paired in these mutants. Yet these *P*-element-derived inserts cause aberrant splicing of sex-specific *fru* transcripts into acceptor sites present within the transposons (Goodwin et al., 2000). This splice-trapping results in anomalous P1-promoted transcripts in Northern blottings stemming from extracts of *fru*^{2}, *fru*^{3}, *fru*^{4}, and *fru*^{sat} adults (Goodwin et al., 2000). In such blots, normal, full-length mRNAs generated by action of P1 were undetectable. However, reverse transcription-PCR assessments were able (with difficulty) to detect low levels of sex-specific *fru*$^+$-like transcripts in males homozygous for a given *fru* variant, although the non-quantitative nature prevented comparison of residual P1-mRNA levels among the four mutant types (Goodwin et al., 2000). In any case, these results suggest that some sex-specific *fru*$^+$ transcripts bypass the aberrant splicing caused by the insertions. Therefore, FRU^M might be detectable in certain of these mutants.

However, none of these issues regarding the male-specific FRU protein has been empirically examined in the *fru* transposon mutants. Thus, in a given mutant, how much, if any, FRU^M would be detectable, and where would it be found within the CNS? To address these matters, anti-FRU^M immunohistochemistry was performed on the CNSs of 2-d-old male pupae and adults carrying the transposon mutations. A principal goal was to correlate FRU^M expression levels with the behavioral impairments of mutants, which are summarized in Table 2. For example, we suspected that this protein would be present at least in *fru*^{2} because such males exhibit the mildest courtship abnormalities among the four transposon mutants used in this study (Table 2).

Homozygous mutants and those heterozygous for a transposon insert and a given recessive-lethal *fru* variant were tested by CNS dissections and application of anti-FRU^M (Figs. 2*B*, 3, 4; Tables 1, 2). *fru*^{2} males exhibited readily detectable staining. In this fertile *fru* mutant (Gailey and Hall, 1989), there were only mild (and less than across-the-board) reductions in numbers of FRU^M neurons, compared with the array of signals observed in the CNS of normal males (Fig. 3, compare *F* with *A, B*) (Table 3). The immunohistochemical signals were 30–40% lower than normal in pupal and adult CNS specimens from *fru*^{2} males (Fig. 3*F*; Table 2). Therefore, the absence of readily detectable P1 transcripts (in Northern blots) is especially misleading for this mutant.

Table 2. Staining intensities of FRU^M-expressing cells in *fruitless* mutants

Genotype (Sex)	Behavioral changes	% Relative staining intensity (digitized value ± SEM)			Remarks on staining patterns
		n:Pu/Ad	Pupa	Adult	
WT (M)	N.A.	5/5 or 1	100 (232 ± 5[a], 235 ± 4[b], 236 ± 2[c])	100 (150 ± 12[a], 130[c])	Twenty clusters of FRU^M-containing neurons, within several discrete brain regions and throughout most of the VNC; all cells show similar levels of immunostaining
WT (F)	N.A.	5/6	0	0	No immunoreactive cells visible
fru^1 (M)	Court F; sings; sterile; vig. M-M	7/5	24 (55 ± 9[a]), 21 (49 ± 8[b]), 100 (235 ± 12[c])	92 (120 ± 11[c])	Staining intensities variable among immunoreactive cells; levels of FRU^M normal or nearly so in several cells, but reduced in most, including to 0 in *fru*-mAL and ASP1 cluster (Fig. 4); ectopic expression in many non-FRU^M cells within brain and VNC (Fig. 4)
fru^2 (M)	Court F; sings; fertile; mild M-M	5/5	67 (156 ± 3[a])	60 (89 ± 7[a])	Non-severe and apparently uniform decrement in staining intensity
fru^3 (M)	Weak court F; mute; sterile; mild M-M	5/5	0	0	No immunoreactive cells visible
fru^4 (M)	Court F; mute; sterile; mild M-M	5/5	4 (9 ± 1[b])	0	A few immunoreactive cells visible with extremely low intensities in *fru*-P and pSP2 clusters (Fig. 3)
fru^{sat} *(M)*	Very weak court F; mute; sterile; mild M-M	5/5	9 (20 ± 2[b])	0	Immunoreactive cells visible with low signal intensities in *fru*-aSP3, Lv, AL, P, SP brain cluster; and PrMs, MsMt, and Ab VNC ones (Fig. 3)

In the genotype column, M designates male and F designates female. The behavioral column briefly summarizes the defects and anomalies reported for these five fruitless mutants by Villella et al. (1997) and Goodwin et al. (2000). N.A., Not applicable; court (or weak court) F, mutant male courts females (or does so weakly as the case may be); mute, performs wing extension when oriented toward or following female, but produces no courtship song; vig. (or mild) M-M, mutant males court each other vigorously (or at relatively low levels, but above that of wild-type inter-male courtship-like interactions). For the immunohistochemical results tabulated here, brains were dissected from animals at two life-cycle stages: 2-d-old pupae and 4 to 7-d-old adults. In the *n* column, numbers of pupal specimens (Pu) are indicated on the left, numbers of adult brains (Ad) on the right. For wild-type (WT) and *fru*^{1} pupae, immunostaining levels in the brain-neuronal clusters *fru*-aSP2, *fru*-P, and *fru*-mcAL (Figs. 3, 4*A,C,E*) were analyzed. The *fru*^{1} mutant showed variable staining intensities among cells or within clusters, as shown in Figure 4; here, this variability is exemplified by quantifying FRU^M levels in three brain-cell groups of pupae and one such (*fru*-mcAL) in adults. For *fru*^{2} pupae and adults, the comparisons relative to WT are for the *fru*-aSP2 cluster. For *fru*^{4} and *fru*^{sat}, cells in *fru*-P clusters were analyzed (Fig. 3*H,I*), these being one of only two brain regions retaining FRU^M immunostaining in these mutants (in pupae only). The mean digitized signal levels (± SEM) are within parentheses in the first two data columns (no SEM for *fru*-mcAL in WT adult, in that only one specimen was quantified for this cluster, whereas five WT male brains were analyzed for *fru*-aSP2). The nominal maximal values for wild-type pupal and adult brains were set at 100%, and the mutant percentages quoted are relative to that maximum.

[a] *fru*-aSP2.

[b] *fru*-P.

[c] *fru*-mcAL.

The other three transposon mutants are sterile and exhibit more severe courtship defects than does *fru*^{2} (Villella et al., 1997; Goodwin et al., 2000; Nilsson et al. 2000). We suspected that at least one of these behaviorally sterile mutants, such as *fru*^{sat}, which is nearly courtless, might be a FRU^M-null variant. In the immunohistochemical assays, however, *fru*^{sat} showed small numbers of cells, albeit with extremely low levels of staining; the results from *fru*^{4} were similar (Fig. 3*H,I*; Table 3). Such minimal signals were in partly overlapping regions of the CNS of these two mutants: in brain clusters called *fru*-pSP2 and *fru*-P (Fig. 3, compare *H, I* with *A–C* for wild type; also see Tables 2, 3). In addition to *fru* expression in these two portions of *fru*^{sat} brains, weakly stained neurons were found in three anterior brain regions *fru*-aSP3, Lv, and AL) as well as in certain ventral cord regions: *fru*-PrMs, MsMt, and Ab clusters (Fig. 3, compare *C*, *I*; see also Tables 2, 3). In the VNC of pupae, *fru*^{4} was blank. No staining was detected in the CNS of *fru*^{sat} or *fru*^{4} adults. The effects of *fru*^{3} were the most severe because no confocally observable immunohistochemical signals were observed in the CNS of either pupae or adults (Fig. 3*G*; Tables 2, 3). The absence of detectable FRU^M in *fru*^{3} specimens was also observed in males heterozygous for that mutation and either of two *fru* deletions (Fig. 2*B*).

The final homozygous-viable *fruitless* mutant examined was *fru*^{1}. Such males court females vigorously, although they do not mate with them, and they exhibit by far the most dramatic intermale courtships of all *fruitless* mutant types (Table 2). *fru*^{1} is caused by an inversion breakpoint within the locus (Gailey and Hall, 1989) that is located ~3 kb upstream of the transcription-start site for P1-promoted mRNAs (Fig. 1). In Northern blots of *fru*^{1} extracts (Goodwin et al., 2000), probed with nucleic acids from the same region used in the current *in situ* hybridizations (Fig. 1), all of the usual sex-specific transcripts were present in both sexes of *fru*^{1} homozygotes (there are three such P1-promoted mRNA types because of alternative splicings at the 3′ end of the primary transcripts). However, this mutant exhibited

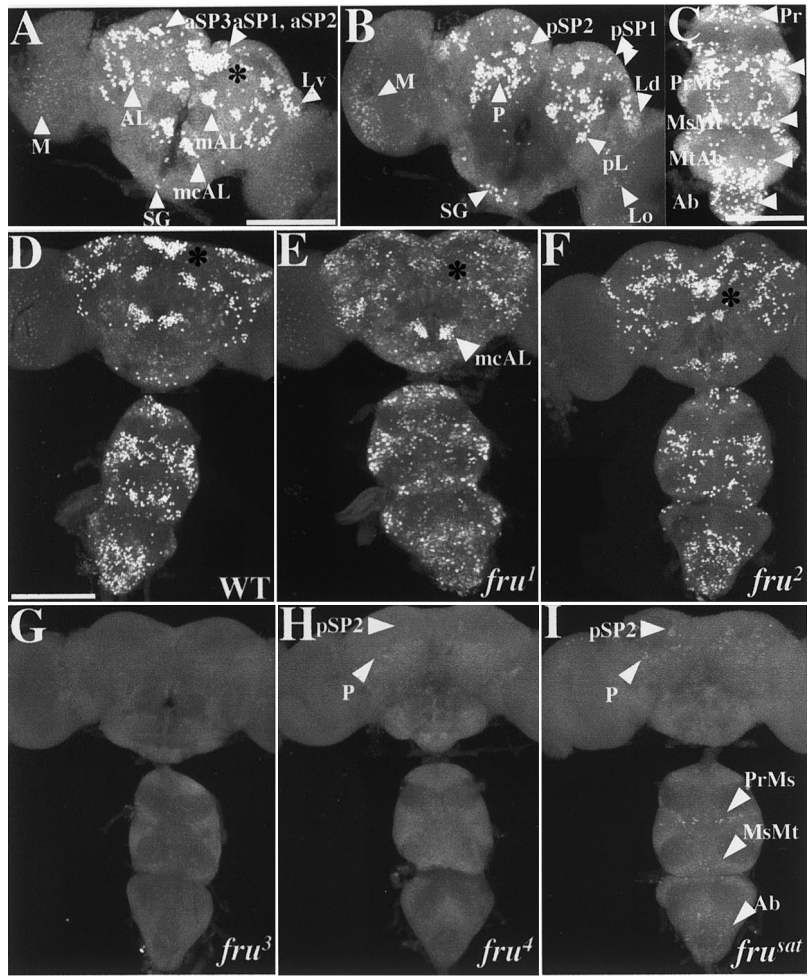

Figure 3. Effects of viable *fruitless* mutations on FRU^M expression in the CNS. Pupal progeny of crosses involving heterozygous male parents (for most of these mutant genotypes, for which homozygosity causes sterility) had CNSs dissected and subjected to immunostaining. All specimens shown are from 2-d-old pupae, the images for which were obtained by confocal microscopy at 20×. The definitions and approximate intra-CNS locations of the FRU^M-expressing neuronal clusters designated by *white arrowheads* (e.g., aSP3, AL, mcAL) are specified in Table 3 (also see Lee et al., 2000). *A*, *B*, Anterior and posterior views, respectively, of wild-type male brains (representative of 36 specimens exposed to anti-FRU^M). *C*, Ventral nerve cord from a wild-type (WT) male, as viewed (in the microscope) from the dorsal side of these ganglia but shown as a projection of stacked optical sections through the whole ventral cord. In *A–C*, groups of FRU^M-containing view of the WT male pattern. CNS neurons are designated by *white arrowheads*. *D*, Overall view of the WT male pattern. This image (and most of those in *E–I*) is a projection from stacked optical sections starting from the anterior side of the brain and the ventral side of the VNC. *E–I*, Similar views of CNSs from pupae homozygous for each of the five viable mutations. These brain-plus-VNC images are representative of the following numbers of specimens: *E*, *fru*^{1} ($n = 7$); *F*, *fru*^{2} ($n = 5$); *G*, *fru*^{3} ($n = 15$); *H*, *fru*^{4} ($n = 5$); and *I*, *fru*^{sat} ($n = 5$). Two nearby dorsal brain clusters, *fru*-aSP1 and *fru*-aSP2 (see *A*), have signal-containing locations indicated by *asterisks* in *D–F*. *H*, *I*, The *arrowheads* near the top point to the locations of a few brain cells (compared with WT) that stained within two brain groups (cf. *B*) of these two mutants. *I*, The three *arrowheads* at the *bottom* point to a few VNC cells that stained within the *fru* thoracic- and abdominal-ganglionic groups (cf. *C*). Scale bars, 100 μm.

anomalies in the spatial expression of P1 transcripts examined in the CNS of pharate adults (Goodwin et al., 2000). It is as if the chromosomal lesion in *fru*^{1}, which occurred in a 5′-flanking region of the locus (Fig. 1) and thus may have damaged regulatory sequences, causes qualitatively altered expression of sex-specific mRNAs at the level of transcription. This is in contrast to the effects of the transposon mutations, the effects of which are post-transcriptional (see above).

Immunohistochemical results from CNSs of 2-d-old pupal males homozygous for *fru*^{1} are shown in Figures 3*E* and 4 and summarized in Tables 2 and 3. Major differences were observed when compared with the wild-type pattern. First, certain clusters, or neurons within a given cluster, were absent in the CNS of the *fru*^{1}. In particular, regions *fru*-mAL and aSP1 were devoid of staining. Other brain regions that are stained by anti-FRU^M in wild-type males, such as *fru*-aSP3, Lv, and mcAL, had reasonably clear signals in corresponding portions of *fru*^{1} brains (Fig. 4, compare *A*, *C*). Second, most of the FRU^M neurons of this mutant showed weaker staining intensity when compared with that of wild type. However, few cells, in particular within the *fru*-aSP3 and *fru*-Lv brain clusters, exhibited nearly normal levels of FRU^M immunostaining (Fig. 4*A–D*). Third, another difference from the norm involves novel cells within the *fru*^{1} brain that express the male-specific protein (Fig. 4*H*). Such ectopic expression of FRU^M within numerous cells of the CNS made it difficult to determine whether certain normal clusters or cells in a given cluster are missing in *fru*^{1}. The three kinds of *fru*^{1} versus wild-type differences just enumerated were also observed in the ventral CNS of male pupae (Fig. 4*I*,*J*). Also, *fru*^{1}-associated reductions in numbers of neurons were discernible in most of the VNC clusters, such as *fru*-Ab, PrMs, and MsMt (Fig. 4*I*,*J*,*K*). In the *fru*^{1} abdominal ganglion, FRU^M immunostaining (within the relevant *fru*-Ab) neurons was diminished (Fig. 4, compare *I*, *J*). This is dealt with in more detail in the next section.

These immunohistochemical results from the five viable *fru* mutants permit certain rationalizations of variations among their extents and types of courtship defects. These mutants can be categorized into two groups. One consists of *fru*^{1} and *fru*^{2}, which court rather vigorously (Table 2). These mutants exhibited decrements in FRU^M expression in the CNS, but overall are nowhere near the amorphic state for P1-encoded proteins. *fru*^{1} showed strong immunohistochemical decreases in certain FRU^M neurons, whereas *fru*^{2} was more uniformly hypomorphic. The other mutant group consists of *fru*^{3}, *fru*^{4}, and *fru*^{sat}, which exhibit no FRU^M expression or immunostaining in very small numbers of neurons. These three sterile mutants court females at lower to much-lower levels than those characteristic of *fru*^{1} and *fru*^{2} male behavior (Table 2).

Subnormalities of FRU^M expression in the VNC of *fru* mutants are likely to be connected with their courtship-song defects. In this regard, *fru*^{sat} males, which are mute (Goodwin et al., 2000), exhibited thoracic-ganglionic FRU^M signals in only a few neurons of the prothorax and mesothorax. The residual VNC expression in this mutant is insufficient for singing to occur. The

Table 3. Counts of FRU^M-expressing cells in the pupal CNS of *fru* mutants

Neuronal cluster	WT	*fru^2*/*fru^2*	*fru^3*/*fru^3*	*fru^4*/*fru^4*	*fru^{sat}*/*fru^{sat}*	*fru^1*/*fru^3*	*fru^1*/*fru^4*	*fru^1*/*fru^{w24}*
Anterior brain								
fru-aSP1	16 ± 1	16 ± 1 (4)	0 (10)	0 (4)	0 (4)	**7 ± 1** (5)	**6 ± 1** (3)	0 (4)
fru-aSP2	57 ± 2	44 ± 3 (5)	0 (10)	0 (4)	0 (4)	**19 ± 1** (5)	**28 ± 1** (3)	**16 ± 1** (4)
fru-aSP3	40 ± 3	36 ± 2 (4)	0 (10)	0 (4)	5 ± 1 (3)	**24 ± 3** (5)	**38 ± 1** (3)	**6 ± 2** (3)
fru-Lv	17 ± 1	18 ± 1 (4)	0 (10)	0 (4)	5 ± 2 (2)	15 ± 1 (5)	20 ± 4 (3)	**9 ± 1** (4)
fru-mAL	29 ± 1	22 ± 1 (4)	0 (10)	0 (4)	0 (4)	**7 ± 1** (5)	**10 ± 2** (3)	**1 ± 1** (3)
fru-AL	54 ± 3	46 ± 1 (5)	0 (10)	0 (4)	9 ± 2 (4)	46 ± 4 (7)	50 ± 2 (4)	**29 ± 6** (2)
fru-mcAL	30 ± 1	25 ± 4 (2)	0 (10)	0 (4)	0 (4)	32 ± 2 (5)	33 ± 2 (4)	27 ± 2 (3)
Spanning portions of both anterior and posterior brain								
fru-SG	12 ± 1	16 ± 2 (4)	0 (10)	0 (4)	0 (4)	7 ± 1 (3)	9 ± 2 (4)	7 ± 4 (2)
fru-M	164 ± 8	N.A.	0 (10)	0 (4)	0 (4)	N.A.	N.A.	N.A.
fru-Ld	50 ± 4	N.A.	0 (10)	0 (4)	0 (4)	N.A.	N.A.	N.A.
fru-Lo	34 ± 1	N.A.	0 (10)	0 (4)	0 (4)	N.A.	N.A.	N.A.
Posterior brain								
fru-pSP1	7 ± 1	7 ± 1 (2)	0 (10)	0 (4)	0 (4)	6 ± 1 (3)	7 ± 1 (4)	4 ± 1 (3)
fru-pSP2	16 ± 1	16 ± 2 (4)	0 (10)	4 ± 1 (4)	7 ± 1 (3)	15 ± 2 (3)	14 ± 1 (4)	**6 ± 2** (2)
fru-P	73 ± 4	62 ± 1 (4)	0 (10)	5 ± 1 (4)	20 ± 4 (4)	87 ± 13 (3)	76 ± 4 (4)	59 ± 6 (2)
fru-pL	12 ± 2	11 ± 2 (4)	0 (10)	0 (4)	0 (4)	11 ± 2 (3)	12 ± 2 (5)	14 ± 1 (2)
Thoracic ganglia								
fru-Pr	21 ± 1	17 ± 1 (4)	0 (10)	0 (4)	0 (4)	15 ± 1 (4)	14 ± 2 (5)	**9 ± 2** (2)
fru-PrMs	83 ± 1	71 ± 1 (4)	0 (10)	0 (4)	10 ± 1 (4)	**49 ± 3** (3)	**57 ± 3** (3)	**31 ± 2** (2)
fru-MsMt	52 ± 4	35 ± 2 (4)	0 (10)	0 (4)	4 ± 1 (4)	**25 ± 3** (3)	**29 ± 2** (3)	**27 ± 9** (2)
fru-MtAb	14 ± 1	8 ± 2 (4)	0 (10)	0 (4)	0 (4)	10 ± 1 (3)	11 ± 1 (3)	14 ± 2 (3)
Abdominal ganglion								
fru-Ab	91 ± 3	83 ± 2 (4)	0 (10)	0 (4)	8 ± 1 (4)	**44 ± 2** (3)	**49 ± 5** (3)	**24 ± 3** (3)

Immunostaining was mediated by application of anti-FRU^M to the CNS of 2-d-old pupal males of various homozygous or heterozygous *fru* types (including homozygous *fru$^+$* = wild-type = WT). All *fru* variants indicated are mutant alleles except *w24*, which designates a *fru*-locus deletion. Numerical data from the *fru^1* mutant are not included, because there are too many weakly stained, ectopically located cells to count them accurately; and the more intensely labeled cells in the various ganglia of this mutant (putative subsets of the WT patterns) could not necessarily be distinguished on a cell-by-cell basis from those with "weak" signals (Figs. 3–5). Numbers (mean ± SEM) of signal-containing neurons were counted within a given neuronal group for one side of the brain or the VNC (see below); *n* values for these hemi-ganglia are in parentheses. The neuronal groupings (leftmost column) were classified as in Lee et al. (2000), and in fact the numbers of FRU^M cells within the various WT neuronal clusters (leftmost data column) are from that report (although in it, results of the cell counts were quoted as mean ± range). The complete absence of staining within a given CNS region is indicated by a "zero" count. For most specimens, counts of immunostained neurons were made for the cluster in question within the left or (bilaterally symmetrical) right side of the brain or ventral nerve cord; when both sides of a CNS were used, the left and right counts were treated independently. Values in **bold** indicate that there was at least an approximately twofold difference between the mean mutant value compared with that of WT (bold not used for the obvious "zero" mutant cases). Despite the appearance (under the microscope) of signal-containing neurons in brain clusters *fru*-M, *fru*-Ld, and *fru*-Lo in three of the mutant types, cell counts were not performed because of extremely low staining levels in these regions for pupae of these genotypes (thus, N.A., data not available).

songless *fru^3* and *fru^4* types provide no putative neural-dissection information because these mutants are devoid of detectable FRU^M throughout the thoracic ganglia. The song-enabled *fru^1* mutant shows approximately one-third of the normal number of FRU^M prothoracic and mesothoracic neurons with ostensibly normal staining intensities; many other such neurons exhibit significantly reduced immunostaining (Fig. 4, compare *I*,*J*), as if they may not be involved in basic singing ability. Adding rather robust *fruitless* expression to these prothoracic/mesothoracic neurons in the *fru^2* mutant, such that these males express FRU^M within the majority of the cells in this VNC region, instead of only one-third of them as in *fru^1*, makes no apparent difference. *fru^2* males sing vigorously but exhibit the same mild defect as do *fru^1* males (Villella et al., 1997).

fru^3, *fru^4*, and *fru^{sat}* males do not attempt copulation and lack a male-specific abdominal muscle called the Muscle of Lawrence (MOL; Gailey et al., 1991; Ito et al., 1996; Villella et al., 1997). The near-to-complete absence of FRU^M abdominal ganglionic signals in these mutants (Table 3) is likely to underlie such defects. Some information is provided as to which abdominal neurons may differentially control these two phenotypes, in that *fru^{sat}* males retain a small proportion of the normal abdominal ganglionic pattern, but such FRU^M cells are insufficient for any MOL formation or abdominal bending toward the genitalia of the female. However, there is a problem with one element of this supposition: the overall courtship of *fru^{sat}* males, and that of *fru^3* as well, is so diminished beyond the early orientation and female-following stages (Villella et al., 1997; Goodwin et al., 2000) that the absence of a late-stage behavior such as attempted copulation is not as meaningful as in the case of a vigorous mutant courter. Thus, the courtship performed by *fru^1* males, for which attempted copulation is also utterly absent, is potentially more interesting in this regard, an issue taken up in the next section. With regard to the abdominal MOL, *fru^1* possesses these male-specific structures, albeit in diminished form (Gailey et al., 1991). MOL formation during the metamorphosis of this mutant is likely to be controlled by certain of the relatively few neurons that robustly express the protein in *fru^1* abdominal ganglia (Fig. 4; cf. Lawrence and Johnston, 1986; Currie and Bate, 1995). *fru^2* causes MOL abnormalities as well (Gailey et al., 1991), but it is less quantitatively subnormal in abdominal ganglionic expression of FRU^M compared with *fru^1* (let alone the severely depleted

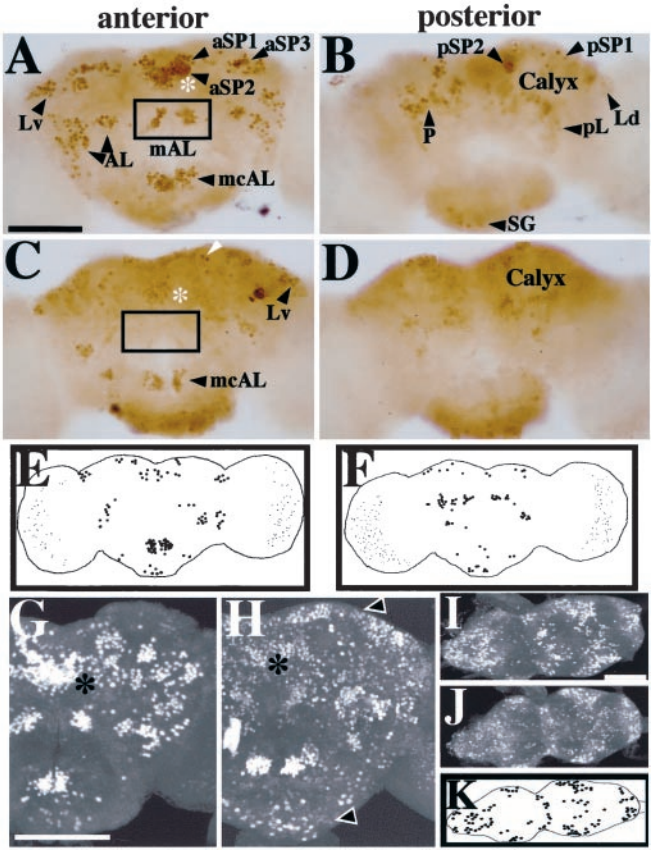

Figure 4. Nonrandom spatial effects of *fru*^{1} on expression of FRU^M in the brain. Pupal progeny of males heterozygous for this (recessive sterilizing) mutation had CNSs dissected (from 2-d-old pupae) and subjected to whole-mount anti-FRU^M histochemistry. *A*, *B*, Control brightfield micrographs (from PhotoShop assemblies of four to five consecutive focal-plane images each) obtained from a wild-type (WT) brain, representative of 20 specimens stained by peroxidase-mediated color reactions (Fig. 3, compare *A*, *B*). *C*, *D*, *fru*^{1} anterior- and posterior-brain patterns, respectively, from scrutiny of 12 mutant specimens (processed and photographed as in *A* and *B*). Only a few cells with low-intensity staining were detected within the *fru*-aSP1 and *fru*-aSP2 clusters of *fru*^{1} brains (*asterisks,* C vs *A*). *C*, The *boxed area* designates the absence of the normally stained *fru*-mAL cluster (cf. box in *A*). Certain neurons showed no apparent staining-intensity decrement compared with WT; this is exemplified by neurons pointed to by *arrowheads* in *C* (also see *E* and *F*). Other FRU^M cells or clusters were absent or exhibited significantly decreased staining intensities in this mutant, e.g., in the vicinity of the mushroom-body *calyx* (*D*); these qualitative and quantitative anomalies of sex-specific *fru* expression are consistent with those obtained by *in situ* hybridizations using later-stage *fru*^{1} pupae (Goodwin et al., 2000). *E*, *F*, Diagrams of representative anterior and posterior *fru*^{1} brain views, respectively, showing cells or clusters with relatively strong staining intensities in brain regions that apparently correspond to those expressing FRU^M in WT. *G*, *H*, Confocal images showing, respectively, anterior views of 2-d-old male pupal brains from WT and *fru*^{1} males (representative of 36 and 7 specimens, respectively, processed in this manner for animals of the two genotypes). *Asterisks* denote the location of the nearby *fru*-aSP1 and *fru*-aSP2 clusters that exhibit subnormal numbers and intensities of stained neurons in *fru*^{1} (*H*). Brains from this mutant also contain FRU^M immunostaining in regions not labeled in WT. Such ectopic signals in *fru*^{1} are widely distributed and show low-intensity staining. *Arrowheads* point to examples of such ectopic-expression regions. *I*, *J*, Confocal images showing ventral views of ventral nerve cords dissected from WT and *fru*^{1} 2-d-old male pupae. *K*, Diagram of FRU^M-containing VNC neurons that gave relatively high-intensity staining. These cells are in posterior CNS regions that apparently correspond to the locations of such neuronal groups, although numbers of signal-containing cells are reduced within a given VNC region of the mutant. Scale bars, 100 μm.

transposon mutants). However, a spatially nonrandom subnormality in a few of the CNS cells may be sufficient to impinge on MOL formation in *fru*^{2}. Despite the mild and generalized FRU^M decrements in *fru*^{2} (Table 2), including within the VNC, these males routinely attempt copulation.

Perhaps the most dramatic courtship anomaly exhibited by a *fruitless* mutant involves the fact that *fru*^{1} males court other males in an extremely vigorous manner, compared with the levels of such "courtship chaining" behavior that are caused by any of the other mutations, let alone the complete absence of such behavior in groups of wild-type males (Villella et al., 1997). It is reasonable to presume that the neural etiology of courtship chaining (and the anomalously high levels of inter-male courtships observed when two *fruitless* individuals are paired) is in the brains of the mutants. The abnormalities of FRU^M expression in that part of the CNS are also unique in *fru*^{1}, in the sense that several brain regions exhibited nearly normal distributions and apparent levels of the protein, but a limited number of other regions showed severe decrements in staining (Table 2; Fig. 4). A comparison of the FRU^M brain-expression pattern in *fru*^{1} with the more severe and global decrements in staining observed for certain of the other mutantsprovides an explanation for the dramatically varying degrees of sex-recognition breakdown among the different *fruitless* mutants (see Discussion).

FRU^M in semifertile *fru*-mutant transheterozygotes

Males homozygous for *fru*^{1}, *fru*^{3}, or *fru*^{4} do not attempt copulation and are sterile; but *fru*^{1}/*fru*^{3} and *fru*^{1}/*fru*^{4} males are fertile, albeit in lower than normal proportions (Castrillon et al., 1993; Villella et al., 1997). To examine whether the ability of the transheterozygous males to bend their abdomens toward the female's genitalia correlate with novel FRU^M-expression phenotypes, immunohistochemistry on whole-mounted CNSs was performed. Tissues were dissected from 2-d-old male pupae of *fru*^{1}/*fru*^{3} or *fru*^{1}/*fru*^{4} and compared with specimens from wild type, the parental homozygous types, and *fru*^{1}/*Df-fru*^{w24}; the latter type is heterozygous for the *fru*^{1} mutation and a complete deletion of the locus, a genotype that causes male behavioral sterilty (Anand et al., 2001).

Several interesting FRU^M immunostaining differences were revealed among these mutant types. First, there was an ~30% decrease in apparent protein expression levels in the transheterozygotes compared with wild type (Fig. 5, examples of quantified results in legend). FRU^M levels in the sterile *fru*^{1}/*Df-fru*^{w24} male type were apprehended to be as low as in *fru*^{1}/*fru*^{3} and *fru*^{1}/*fru*^{4} (staining intensities not quantified for *fru*^{1}/*Df-fru*^{w24}). Overall expression levels seemed to be uniform throughout CNS in the three heterozygous types just described. Second, there were marked reductions in the numbers of stained cells in several clusters within the CNS of *fru*^{1}/*fru*^{3} and *fru*^{1}/*fru*^{4} males, such as *fru*-aSP1, aSP2, aSP3, mAL (brain), *fru*-PrMs, MsMt, and Ab (ventral nerve cord) (Fig. 5). Depending on the neuronal group (among the seven just indicated), the number of FRU^M cells decreased approximately two- or threefold (Table 3). In other CNS regions, the numbers of stained neurons were nearly normal (Table 3). The reductions, or lack thereof, were quite consistent when comparing the signals and counts from *fru*^{1}/*fru*^{3} to those from *fru*^{1}/*fru*^{4} (Fig. 5; Table 3). Third, anti-FRU^M staining patterns for these *fru*^{1}/*fru*^{3} and *fru*^{1}/*fru*^{4} males were somewhat similar to those of *fru*^{1} homozygotes. The distributions of signal-containing neurons in these transheterozygotes resembled those of strongly stained cells in males homozygous for *fru*^{1} (Fig. 4,

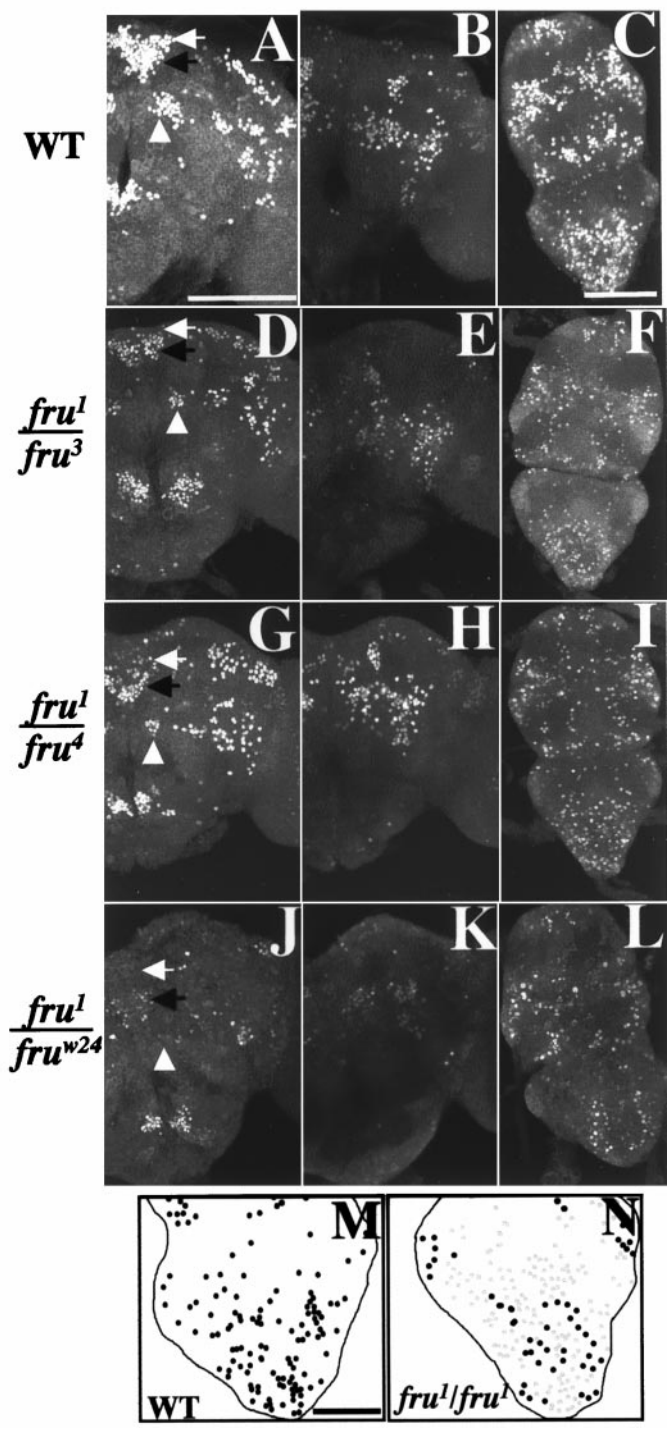

Figure 5. FRU^{M} expression in the CNS of quasi-fertile *fruitless* mutant combinations. CNSs from 2-d-old male pupae carrying *fru*^{1}/*fru*^{3} ($n = 14$), *fru*^{1}/*fru*^{4} ($n = 12$), wild type (WT, $n = 36$), and *fru*^{1}/*Df-fru*^{w24} ($n = 6$) were subjected to anti-FRU^{M} immunohistochemistry. WT and *fru*^{1}/*Df-fru*^{w24} were used as normal and fully mutant controls, respectively. The resulting representative images were prepared with confocal microscopy to show both anterior and posterior views of the brain and whole projection of the VNC for WT (*A–C*), *fru*^{1}/*fru*^{3} (*D–F*), *fru*^{1}/*fru*^{4} (*G–I*), and *fru*^{1}/*Df-fru*^{w24} (*J–L*). *A*, *D*, *G*, *J, White arrows, fru*-aSP1 neuronal cluster; *black arrows*, *fru*-aSP2; and *white arrowheads*, *fru*-mAL. *fru*^{1}/*fru*^{3} and *fru*^{1}/*fru*^{4} samples were stained with relatively low intensities overall; for example, the *fru*-aSP2 cluster of FRU^{M}-containing brain neurons in *fru*^{1}/*fru*^{3} and *fru*^{1}/*fru*^{4} males (*D*, *G, black arrows*) gave staining intensities (see Materials and Methods) of 160 ± 14 (mean ± SEM; $n = 3$) and 164 ± 9 ($n = 3$), respectively, whereas the corresponding WT value for compare with Fig. 5*J*, *K*, *L*). However, weakly stained FRU^{M} cells (and ectopic ones, see below) were not detectable in *fru*^{1}/*fru*^{3} or *fru*^{1}/*fru*^{4} males.

Now we focus on abdominal ganglion expression of FRU^{M} in fertile *fru*^{1}/*fru*^{3} and *fru*^{1}/*fru*^{4} males compared with sterile *fru*^{1}/*fru*^{1} and *fru*^{1}/*Df-fru*^{24} males, against a background of the likelihood that the male's copulation attempts are controlled by this posterior-most region of the CNS. In the abdominal ganglion, ~50% of the normal numbers of FRU^{M} cells were stained in *fru*^{1}/*fru*^{3} and *fru*^{1}/*fru*^{4}, and ~25% in *fru*^{1}/*Df-fru*^{w24} males (Table 3). This difference in the FRU^{M} cell number might be responsible for the lack of attempted copulation by *fru*^{1}/*Df-fru*^{w24} males. However, the twofold decrement in the transheterozygotes (compared with wild-type) is still compatible with routine mating ability. These *fru*^{1}/*fru*^{3} and *fru*^{1}/*fru*^{4} males did not show any ectopic expression of FRU^{M}, of the kind that *fru*^{1} homozygotes exhibit in the abdominal ganglion (Fig. 5, compare *N*,*M*) as well as in other CNS ganglia (see previous section of Results). This homozygous-sterile mutant type also exhibits a decrement in the number of heavily staining abdominal ganglionic neurons (Fig. 5, *N* vs *M*; compare Fig. 3, *E* vs *D,* and Fig. 4, *J* vs *I*) similar to the paucity shown by *fru*^{1}/*Df-fru*^{w24} males (see above; Fig. 5, compare *L*,*N*).

In general, the three male types that each carried only one copy of the *fru*^{1} mutation gave protein-expression patterns similar to one another, although *fru*^{1}/*Df-fru*^{w24} hemizygous males were farther from wild type, compared with the fertile but FRU^{M}-subnormal transheterozygotes (Fig. 5; Table 3). Nevertheless, the similarities among *fru*^{1}/*fru*^{3}, *fru*^{1}/*fru*^{4}, and *fru*^{1}/*Df-fru*^{w24} could be explained by an allele-dosage effect. The *Df-fru*^{24} deletion generates no gene product, and homozygosity for *fru*^{3} or *fru*^{4} eliminates most or all FRU^{M} expression (Fig. 3). Thus, FRU^{M} production in the three heterozygous types being considered would seem mostly to come from the one dose of the *fru*^{1} allele in common among them. One reason for the perception of an overall reduction of FRU^{M}, under the influence of this mutation, could be that the weak and ectopically expressing neurons found in *fru*^{1} homozygotes are below detection levels in each of the (one-dose) heterozygotes. However, this *fru*^{1}-dosage effect does not explain why more FRU^{M} cells were observed and counted within certain CNS regions of the *fru*-mutant transheterozygous types, compared with the near absence of staining in *fru*^{1} homozygotes, e.g., for the *fru*-aSP1 and mAL brain clusters. About one-third to one-half the normal numbers of stained neurons were observed in these locations within the CNS of *fru*^{1}/*fru*^{3} or *fru*^{1}/*fru*^{4} males (Fig. 5; Table 3), whereas almost no cellular signals were detected in the corresponding brain regions of *fru*^{1}/*fru*^{1} males (Fig. 4). Therefore, another factor that may point to an explanation of the differences among these three types, which are

←

*aSP2 (*black arrow *in* A*) was 217 ± 7 (*n *= 3). However, the micrographs shown do not reflect such staining-intensity differences, because these confocal images were in saturation to maximize viewability of signal-containing CNS regions.* M, N*, Drawings of fluorescent signals viewed confocally from the ventral side* of the abdominal ganglion to produce both representative diagrams for WT and *fru*^{1}-homozygous males, respectively. In *fru*^{1}/*fru*^{1}, fewer cells than normal stained in a relatively intense WT-like manner (*black dots*); other neurons, possibly representing further subsets of the normal pattern but including many ectopically expressing cells, stained weakly (*gray dots*). These numerous ectopic expressing cells could not be revealed in the low-magnification micrographs for this CNS region in this mutant (Figs. 3*E*, 4*J*). Scale bars: *A–L*, 100 μm; *M*, *N*, 50 μm.

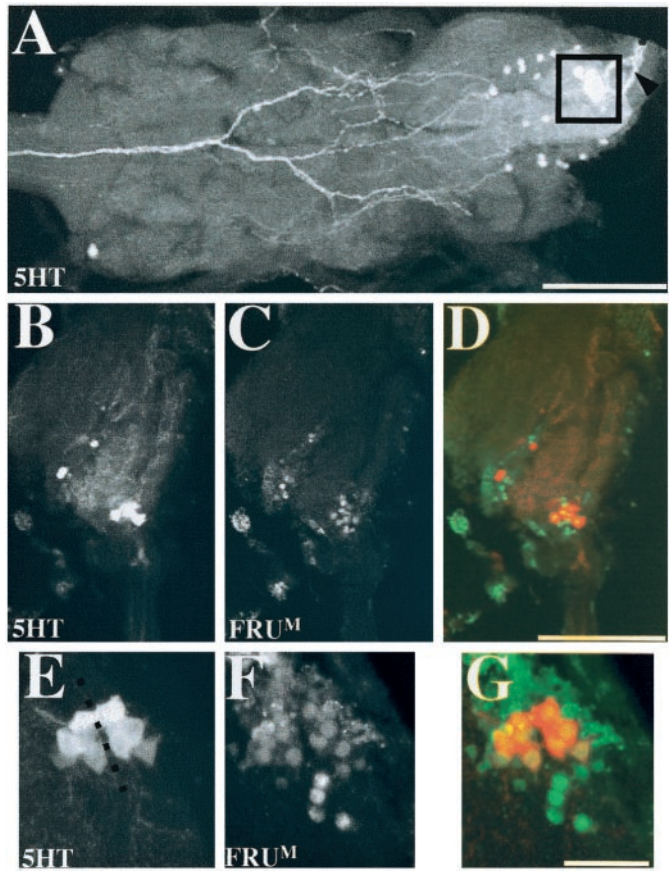

Figure 6. Neurons coexpressing FRU^M and serotonin in the abdominal ganglion. These cells, dubbed s-Abg, were revealed in the posterior tip of the male VNC by anti-5-HT single-labeling and double-labeling application of that antibody along with anti-FRU^M. Twelve 4- to 7-d-old wild-type males were used for anti-5-HT immunohistochemistry alone and 10 separate such males for double-labeling. *A*, Confocal image showing a dorsal view of serotonergic neurons in the thoracic and abdominal ganglia. Two different sizes of anti-5-HT-labeled neurons appear in the abdominal ganglion; the *boxed area* shows a cluster of eight s-Abg neurons; the *black arrowhead* points to the proximal portion of axons projecting posteriorly from these cells into the median trunk nerve. *B*, *C*, Neurons expressing 5-HT- and FRU^M neurons in an adult-male abdominal ganglion. These sagittal views of the s-Abg neurons show the cell bodies to be located dorsally (toward the *right* of each panel). *D*, Combined image of *B* and *C*, depicting coexpression of the two antigens. 5-HT immunoreactivity was observed mostly within (and throughout) the cell bodies (red), and FRU^M immunoreactivity was detected only in nuclei (*green*). *E, F*, Higher-magnification dorsal view of s-Abg neurons labeled by anti-5-HT and anti-FRU^M, respectively. Six consecutive 1.2 μm focal planes were combined to show all s-Abg neurons; the *dotted line* in *E* was drawn to indicate the symmetrically paired structure of the s-Abg neuronal clusters. *G*, Combined image of *E* and *F* (5-HT in *red*, FRU^M in *green*). Scale bars: *A–D*, 100 μm; *E–F*, 25 μm.

most dramatic in terms of fertility, is that there are special kinds of gene interactions between the *fruitless* alleles themselves when *fru*^{1} is heterozygous with *fru*^{3} or *fru*^{4}. This kind of phenomenon would involve something other than the amount of final gene product (in this case male-specific FRU protein) produced according to the dosage of the mutant alleles in question. Instead, as suggested originally by Castrillon et al. (1993), some sort of mutual correction may occur between the alleles on the separate third chromosomes at the level of primary gene expression in *fru*^{1}/*fru*^{3} and *fru*^{1}/*fru*^{4} males. There is, however, no way that a current understanding of the primary transcripts or the array of mature mRNAs encoded by this gene (Ryner et al., 1996; Goodwin et al., 2000) can rationalize the complementing manner by which these mutant alleles may interact.

fru effects on sexually dimorphic serotonergic abdominal cells

To examine the possible relationship between *fruitless* function and 5-HT (see introduction), we double-labeled whole-mounted CNSs with antibodies against FRU^M and the neuromodulator. The results are presented in Figure 6. We found 5-HT-immunoreactive neurons broadly distributed throughout the brain (n = 12, data not shown), the thoracic ganglia, and the abdominal ganglion of adult males (Fig. 6*A*). Previously, Vallés and White (1986, 1988) identified nine groups of serotonergic neurons in the adult brain and five groups in the ventral nervous system of *Drosophila* [see Nässel (1988, 1996) and Monastrioti (1999) for reviews of serotonergic labeling in the CNS of this and other insects]. Against this background, we stained serotonergic neurons in the CNS of adult flies that were genetically normal, compared with those expressing *fru* mutations.

We assume that *fruitless* mutations and ectopic expression of the *white* gene (Zhang and Odenwald, 1975) cause males to court other such flies because of anomalous brain function (possible involvement of the VNC is counterintuitive). Ectopic expression (and probably overexpression) of w^+ in the brain could deplete 5-HT levels in cells that normally express the *fru* gene, mutations of which can easily be found to cause a similar neurochemical deficit (see introduction). Thus FRU^M and 5-HT would be coexpressed in at least some of the neurons that normally contain these substances. However, within the brain of wild-type males, no FRU^M neurons whatsoever were double-labeled with anti-5-HT (n = 10, data not shown). The usual locations of cells and processes immunoreactive for this substance were observed (see above). The number of 5-HT neurons is not particularly large, reinforcing the possibility that global uptake of a serotonin precursor throughout the brain could deplete levels of this substance in their usual locations. However, if ectopic expression of w^+ is mechanistically related to *fru*-mutational effects via 5-HT, the current results indicate that there is a need to formulate a hypothesis different from one involving direct intracellular effects of the latter genotypes. Perhaps *white* and the tryptophan transporter it encodes cause this neuromodulator to be anomalously present in FRU^M cells or other neurons that directly interact with them; such effects might derange *fru*-controlled brain functions insofar as sex recognition is regulated. Another possibility, not mutually exclusive, is that ectopic w^+ leads to anomalous 5-HT levels in cells that interact with FRU^M neurons, deranging brain functions that are not directly controlled by *fruitless* but are components of the neural substrates for courtship. In any case, the lack of a simple relationship between *fruitless* gene products and serotonergic neurons, which would have bolstered the notion that both abnormal genotypes cause their courtship effects via 5-HT depletion in the same key brain cells, suggests that ectopic-*white* males are made to behave in a manner that caricatures the phenotype of *fruitless* mutants.

In the course of these double-labeling tests, we scrutinized signals elicited by anti-FRU^M and anti-5-HT in all CNS ganglia. Within the male's ventral cord, the great majority of *fru*-expressing neurons in the four pairs of ganglia (cf. Lee et al., 2000) contained no detectable 5-HT. There was, however, an exception within one VNC region. It involves certain newly identified serotonergic cells in the abdominal ganglion (Fig. 6).

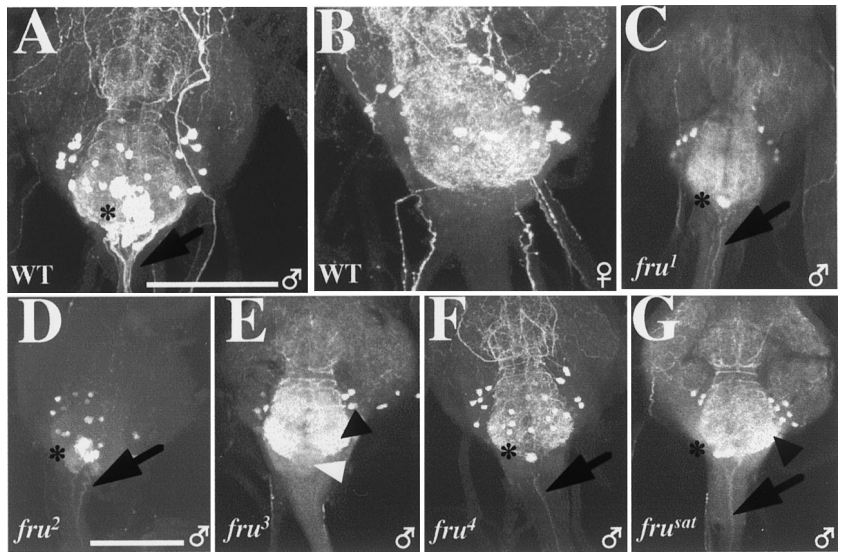

Figure 7. Abnormal sex-specific serotonin expression in the abdominal ganglia of *fru* mutant males. These images are whole (*A*, *B*, *D*, *F*) or partial (*C*, *E*, *G*) projections of stacked images through a given ganglion, viewed in the confocal microscope from the ventral side. *A*, *B*, Abdominal ganglia of 4- to 7-d-old wild-type adult male and female, respectively; in the latter (representative of five female VNCs processed), there were no anti-5-HT-mediated signals like those observed in this region of the male CNS, whose cluster of s-Abg cells (compare Fig. 6) are designated by an *asterisk* in *A* (representative of 12 male VNCs observed); the *arrow* in *A* points to axonal projections from male s-Abg neurons. *C–G*, Serotonergic neurons in the abdominal ganglia of *fru* mutants. *C*, In *fru*^{1} ($n = 5$), s-Abg cell bodies (*asterisk*) and processes (*arrow*) were weakly stained (uniformly among the specimens, in contrast to *fru*^{4}) (see below). *D*, In *fru*^{2} ($n = 8$), the s-Abg neuronal cluster (*asterisk*) and projections from such cells (*arrow*) were normal or nearly so (in terms of numbers of cell bodies and staining intensities) among the several specimens. The image shown depicts strong signals, although in this one there were weak signals in a serotonergic neuropil that usually gives strong staining (*E*, *G*, *black arrowheads*) in abdominal ganglia of all *fru* genotypes (including *fru*^{2}). *E*, In *fru*^{3} ($n = 6$), no 5-HT immunostaining in s-Abg cells or neurites was observed; the *white arrowhead* points to where the cell bodies should be. *F*, In *fru*^{4} ($n = 5$), two specimens showed no 5-HT immunoreactivity in s-Abg neurons, whereas three gave weak staining in one to three s-Abg cell bodies and their processes (as exemplified in the case shown and its *asterisk* for cell bodies and *black arrow* for processes). *G*, In *fru*^{sat} ($n = 5$), relatively few s-Abg neurons were stained by anti-5-HT (although more than in *fru*^{4}), and the cell bodies and processes in which signals were elicited (*asterisk, arrow*) gave weak signals (uniformly among the specimens). Scale bars: *A*, *B*, 50 μm; *C–G*, 100 μm.

For these neurons, coexpression of FRU^{M} and 5-HT was observed in a total of eight cells at the posterior tip of the VNC (Fig. 6). These serotonergic-abdominal giant neurons (s-Abg) are located close to one another in a relatively dorsal side of the abdominal ganglion and have conspicuously large cell bodies (Fig. 6*A–E*). Larval serotonergic neurons in the developing nervous system are reorganized during metamorphosis (Vallés and White, 1988; Monastrioti, 1999). In this respect, putative precursors of the s-Abg neurons were not detected in the third-instar larval CNS ($n = 6$) or in the abdominal ganglion of 2-d-old male pupae ($n = 5$, data not shown). Therefore, these s-Abg neurons in *Drosophila* may form during metamorphosis (cf. Thorn and Truman 1994a,b), or they may have been born earlier and taken on their final neurochemical quality during late stages of development (cf. Tublitz and Sylwester, 1990).

With regard to the projection patterns of the s-Abg cells that were revealed by 5-HT-immunostaining (Fig. 6*A*), each neuron appeared to have more than one neurite. In most specimens, the s-Abg neurons were closely clumped together. A few preparations exhibited fairly clear bilaterality of these cell bodies and their posterior projections. These 5-HT-immunoreactive neurites also appear to be within the median trunk (which is known to innervate posterior abdominal segments), genital segments, and internal reproductive organs (Hertweck, 1931).

The putatively *fru*-related function of these cells and their processes would seem to involve aspects of male reproduction because the patterns of 5-HT immunoreactivity being described were not observed in or posterior to the abdominal ganglion of adult females (Fig. 7, compare *A*, *B*). Whether these cells exist in females, as opposed to being present but devoid of 5-HT, is unknown. In this regard, bear in mind that there is no FRU^{M} immunostaining anywhere in the CNS of females (Lee et al., 2000).

In *fru*-mutant males, anti-5-HT immunoreactivity in the s-Abg neurons as well as the axons projecting from them was absent or defective (Fig. 7). *fru*^{1} and *fru*^{sat} showed low levels of transmitter staining in some of the s-Abg neurons and their process (Fig. 7, *C* and *G*, respectively).

In *fru*^{3}, there was no detectable 5-HT immunoreactivity in s-Abg neurons or their axons (Fig. 7*E*). At best, *fru*^{4} mutant males presented weakly detectable 5-HT immunoreactivity in these structures (Fig. 7*F*). *fru*^{2} males were normal with respect to numbers of s-Abg neurons and their projections (as stained by anti-5-HT), although the levels of staining intensity in both subcellular compartments of these neurons appeared to be lower than in wild type (Fig. 7*D*).

For *fru*^{3}, the most severely subnormal mutant in terms of FRU^{M} and 5-HT expression in the abdominal ganglion, it was not immediately possible to determine whether the general absence of both kinds of immunoreactivity is caused by an absence of s-Abg neurons or by the lack of serotonin production in these cells. To address this question, 5-HT-uptake experiments were performed. These were based on the fact that exogenously applied 5-HT was found to be absorbed selectively by serotonergic neurons in the CNSs of third-instar larvae that expressed late-developmentally lethal *Dopa decarboxylase* (*Ddc*) mutations (Vallés and White, 1988); relatively severe (but viable) *Ddc* variants cause severe decrements in 5-HT synthesis (Livingstone and

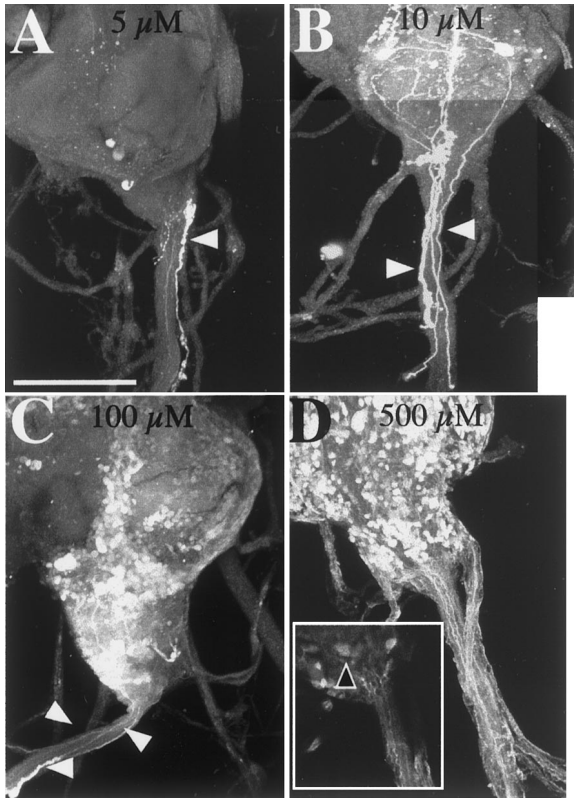

Figure 8. Serotonin immunoreactivity in the abdominal ganglion resulting from exogenous application of 5-HT. Immunohistochemistry with anti-5-HT was performed with dissected VNCs of *fru*^{3} adult males that were incubated in 5-HT solutions. Immunofluorescently labeled tissues were examined by confocal microscopy, and stacked images of abdominal ganglia were obtained from specimens exposed to the range of concentrations indicated. *A–D*, Representative immunostaining after application of 5-HT at 5 μM ($n = 4$) (*A*), 10 μM ($n = 5$) (*B*), 100 μM ($n = 2$) (*C*), and 500 μM ($n = 5$) (*D*). No s-Abg-like 5-HT-immunoreactive neurons or their projections were observed to result from the lowest two concentrations of 5-HT used (*A*, *B*). Thus, the thin neurite signal in *A*, which runs down the center of the median trunk, was traced back to certain cell bodies in the posterior tip of the abdominal ganglion, but they were too small to be s-Abg cell bodies. Another feature of *A* is a cell body and fiber (*white arrowhead*) that appears to be outside of the main abdominal nerve. (In association with these signals are varicosities that suggest the structures are neurohemal fibers that could not be projections from s-Abg cells.) *B*, None of the stained fibers (*white arrowheads*) in the main nerve could be traced back to s-Abg-like cell bodies. *D*, At the highest concentration, a few cells that putatively took up exogenous 5-HT appeared to be similar to s-Abg neurons in their size and shape (*black arrowhead* within the *box*; image of the *box* is based on one focal plane); no such cells exhibit intrinsically derived immunostaining in these cells in this mutant (Fig. 7*E*). The putative s-Abg cell bodies, to which 5-HT was supplied in the *fru*^{3} abdominal ganglion shown (*D*), are in a dorsomedial region of the posterior CNS tip. This is the location of such neurons in more definitively identifiable circumstances (Fig. 7*A*,*C*,*D*). Scale bars, 100 μM.

Tempel, 1983). Ventral nerve cords from adult *fru*^{3} males were exposed to a series of 5-HT-creatinine concentrations ($n = 3$ VNCs at 1 μM, $n = 4$ at 5 μM, $n = 5$ at 10 μM, $n = 2$ at 100 μM, and $n = 5$ at 500 μM). The resulting immunostaining led to the following patterns. In wild-type VNCs ($n = 3$, data not shown), we observed lowered endogenous 5-HT levels in the serotonergic neurons that are undisturbed by this *fru* mutation; we infer that the incubation procedure necessary for 5-HT uptake is the major cause of this depletion. In *fru*^{3} VNCs, at the lowest concentration applied to *fru*^{3} specimens (1 μM, data not shown), neither s-Abg-like cell bodies nor neurites could be recognized; but as incubations with increasing 5-HT concentrations were performed, there were increasing numbers of immunostained cells along with stronger signal strengths (Fig. 8*A–C*). At the highest concentration of 5-HT applied, a subset of these structures in the ganglion of the mutant exhibited what appeared to be the appropriate immunoreactivity (Fig. 8*D*). The signals associated with the VNC cell bodies and processes in question appeared similar to those of genetically normal s-Abgs in their size, shape, and intraganglionic location. Thus, it seems as if at least some of these VNC cells are retained in this mutant and able to take up serotonin. However, it was not possible to determine unambiguously whether the normal *fru*/5-HT-expressing cells and their projections were labeled in the *fru*^{3} ganglia. Therefore, it remains an open question as to whether these neurons are eliminated by a developmental effect of this mutation, or whether, if present, the cells are unable to absorb exogenously applied 5-HT in the conditions used.

DISCUSSION

Correlations between FRU^M expression and *fru*-mutant phenotypes

The various *fruitless* mutants exhibit striking behavioral defects and differences among one another (Goodwin, 1999). The degrees and kinds of anti-FRU^M staining abnormalities found for these five viable mutants were argued (in Results) to correlate with their courtship subnormalities and anomalies. However, the expression/behavioral correlations are not always tight. For example, *fru*^{sat} males are nearly courtless, but they exhibit FRU^M signals in a few cells (Fig. 3*F*). *fru*^{3} males court more vigorously but have no detectable FRU^M (Table 2), equivalent to the effects of chromosome breakpoints within the gene (Table 1). Behaviorally, these breakpoint variants are nearly courtless (Villella et al., 1997; Anand et al., 2001). We suspect that *fru*^{3} males generate low levels of FRU^M protein, more than in the breakpoint variants, but undetectable by the antibody.

A further supposition presented in conjunction with descriptions of the anti-FRU^M results for the viable mutants is that expression defects in relatively posterior regions of the VNC are the neural etiology of the courtship-song abnormalities that are exhibited to one degree or another by all five mutants. It is almost certainly not a coincidence that this sex-specific singing behavior depends on the presence of genetically male neurons in the thoracic ganglia (for review, see Greenspan, 1995).

With regard to FRU^M-immunoreactive neurons in the most posterior region of the VNC, expression defects in the mutants were hypothesized (in Results) to be connected with the inability of four of them (except *fru*^{2}) to attempt copulation, on the one hand, and to develop a normal male-specific abdominal muscle, on the other. The patterns of FRU^M cells in the abdominal ganglia are potentially most interesting for *fru*^{1}/*fru*^{3} and *fru*^{1}/*fru*^{4} males, which are partly fertile (Castrillon et al., 1993; Villella et al., 1997). Many FRU^M-positive cells were observed in the abdominal ganglia of transheterozygotes (Fig. 5), although only ~50% the wild-type number (Table 3). We propose that certain of these neurons regulate attempted copulation. *fru*^{1} homozygotes exhibit fewer abdominal-ganglionic cells that are intensely stained by anti-FRU^M, compared with the transheterozygotes; and males homozygous for this mutation never bend their abdomens to attempt copulation (Hall, 1978). If a certain subset of the FRU^M abdominal ganglionic pattern is critical for this behavior, it could be that such cells are missing or protein-null in *fru*^{1}, yet present in *fru*^{1}/*fru*^{3} and *fru*^{1}/*fru*^{4}. Another possibility is that

ectopic FRU^M cells in the abdominal ganglion in *fru^1* males influence phenotypes involving the abdominal ganglion. In *fru^1*/*fru^3* or *fru^1*/*fru^4* males, no ectopic FRU^M expression was apparent (Fig. 5), which might be the reason for restoration of fertility in the transheterozygotes compared with the behavior of *fru^1* homozygotes (*fru^1*/*Df-fru^{w24}* also showed no ectopic FRU^M neurons, but this is probably a false negative with respect to the detectability of these weakly expressing cells because of the single copy of the functional *fru* allele). In males for which the only *fruitless* allele is *fru^1*, ectopically expressed protein could alter the function of this part of the CNS such that the neuromuscular control of attempted copulation is ruined. This would be a distinctly different etiology than the abdominal-ganglionic FRU^M-lessness (Table 3) that very likely underlies the inability of males homozygous for either *fru^3* or *fru^4* to perform copulation attempts.

Inter-male courtship and FRU^M expression defects

We now consider the expression of *fruitless* in the context of sexual orientation. Wild-type males show female-oriented courtship, whereas *fru* mutants show varying levels of decreased orientation toward females and anomalous interest in other males. *fru^2* is informative in this regard because males homozygous for this mutation prefer females (Villella et al., 1997), and this mutant exhibits the least severe FRU^M expression defects in the brain (Fig. 3*B;* Table 2). However, simple correlations break down for other genotypes. Thus, in single-pair tests, *fru^{sat}* males court other males at lower levels compared with the degrees of homosexual courtships displayed by *fru^3* and *fru^4*; all three of these mutants court other males in group situations at only about one-fourth the level displayed by *fru^1* (Villella et al., 1997; Goodwin et al., 2000). Males homozygous for *fru^3*, *fru^4*, or *fru^{sat}* are similarly depleted of brain FRU^M (Table 2). *fru^1*, the most vigorous courter of other males, cannot have this anomalous behavior explained by gross subnormalities of FRU^M levels. One etiology of the unique inter-male courtship displayed by this mutant may be the ectopically expressing FRU^M neurons found within the brain (discussed above in another context). However, it is also important to consider that *fru^1* males are depleted of the protein nonrandomly (Fig. 4; Table 2). In particular, no FRU^M was detectable within a brain region near the antennal lobes called *fru*-mAL, although a much more dorsal region (aSP1) was also devoid of signals. The part of the brain near (and very likely including) mAL is provocative because this region has been implicated in sexual recognition; genetically feminized brain sites in the vicinity of the antennal lobes cause such males to court other males (Ferveur et al., 1995). The same behavioral effect could result from these brain sites being inadequately masculinized, if that is the consequence of a lack of FRU^M in this region.

The other viable mutants that exhibit homosexual courtship are immunohistochemically similar to *fru^1* in that all lack FRU^M in sites near the antennal lobes (Figs. 3, 4). It is possible that the *fru^3*, *fru^4*, and *fru^{sat}* mutants court other males at relatively low levels compared with the behavior of *fru^1* because the latter mutant retains FRU^M in several brain regions necessary for any courtship. In other words, the brakes would be off in *fru^1*, absent mAL expression of FRU^M (Fig. 4); but the product of the gene must be elsewhere in the brain for that effect to manifest itself in terms of robust inter-male courtship. At least one such region is very likely the dorsoposterior region that does contain FRU^M cells (Lee et al., 2000; and this report) and requires the presence of genetically male neurons in order for any male-like courtship to occur (for review, see Greenspan, 1995). The fact that the *fru^3* mutant courts other flies of either sex more vigorously than do *fru*-deletion males is probably attributable to the (aforementioned) supposition that this transposon mutant generates modest levels of FRU^M, albeit indistinguishably above the zero immunostaining observed in the double-deletion types (Table 1). Their near-courtlessness is consistent with the idea that some FRU^M is required if an appreciable level of male courtship is to be directed toward another fly, be it male or female.

Possible male-specific functions of *fru*-affected serotonergic neurons

Our discovery of sexually dimorphic s-Abg neurons in the abdominal ganglion (Figs. 6, 7) could provide an anatomical link to *fru$^+$*-dependent sex-specific phenotypes not yet known to be influenced by this gene. The s-Abg neurite signals elicited by anti-5-HT also provide the first information on a projection pattern for *fru*-expressing cells. These findings indicate that the formation of the s-Abg neurons or production of 5-HT in them is male-specific and under *fru* control. The 5-HT-uptake results (Fig. 8) suggest that s-Abg cells are present but are unable to synthesize this transmitter in the FRU^M-less *fru^3* mutant.

Innervation by 5-HT/FRU^M neurons of abdominal muscles influenced by *fru*-gene action is unlikely. This is because glutamate is the canonical neuromuscular transmitter in *Drosophila* (e.g., DiAntonio et al., 1999), although comprehensive information is understandably lacking as to whether this molecule is responsible for intercellular communication at all such synapses. In addition to the muscles in this body region, there are male-specific organs that have better-appreciated structures (compared with unknown muscles hypothetically devoted to attempted copulation) and functions (compared with the MOL) for which reproductive significance is unknown. In this regard, the s-Abg neurons seem to send their axonal projections into the median-trunk nerve (Hertweck, 1931), the terminal branches of which innervate the genital segments and internal reproductive organs as well as certain abdominal muscles (Miller, 1950)

5-HT has been suggested to play a role in altered sexual orientation in *Drosophila* (Zhang and Odenwald, 1995). A potentially close connection between the action of FRU^M and serotonin in terms of inter-male courtship would have been worthy of deeper consideration if these factors had been found to be coexpressed. But the current results uncovered no overt 5-HT link to *fru*-expressing brain neurons. The fact that there is a distinctly separate colocalization of FRU^M and serotonin at the opposite end of the CNS (Figs. 6–8) suggests that regulation of the presence and action of this neurotransmitter can be a downstream target of *fru* function, an unexpected connection between the control of sexual differentiation and this piece of *Drosophila* neurochemistry. This bonus was but one of the results of being able to monitor the presence of *fruitless* gene products at high resolution.

REFERENCES

Anand A, Villella A, Morales A, Ryner LC, Carlo T, Goodwin SF, Song H-S, Gailey DA, Hall JC, Baker BS, Taylor BJ (2001) The sex determination gene fruitless, in addition to controlling male sexual behaviors, has sex-nonspecific vital functions. Genetics, in press.

Castrillon DH, Gonczy P, Alexander S, Rawson R, Eberhart CG, Viswanathan S, DiNardo S, Wasserman SA (1993) Toward a molecular genetic analysis of spermatogenesis in *Drosophila melanogaster*: characterization of male-sterile mutants generated by single *P*-element mutagenesis. Genetics 135:489–505.

Currie DA, Bate M (1995) Innervation is essential for the development

and differentiation of a sex-specific adult muscle in *Drosophila melanogaster*. Development 121:2549–2557.
DiAntonio A, Petersen SA, Heckmann M, Goodman CS (1999) Glutamate receptor expression regulates quantal size and quantal content at the *Drosophila* neuromuscular junction. J Neurosci 19:3023–3032.
Ferveur J-F, Störtkuhl KF, Stocker RF, Greenspan RJ (1995) Genetic feminization of brain structures and changed sexual orientation in male *Drosophila*. Science 267:902–905.
Finley KD, Taylor BJ, Milstein M, McKeown M (1997) *dissatisfaction*, a gene involved in sex-specific behavior and neural development of *Drosophila melanogaster*. Proc Natl Acad Sci USA 94:913–918.
Fratta W, Biggio G, Gessa GL (1977) Homosexual mounting behavior induced in male rats and rabbits by a tryptophan-free diet. Life Sci 21:379–383.
Gailey DA, Hall JC (1989) Behavior and cytogenetics of *fruitless* in *Drosophila melanogaster*: different courtship defects caused by separate, closely linked lesions. Genetics 121:773–785.
Gailey DA, Taylor BJ, Hall JC (1991) Elements of the *fruitless* locus regulate development of the muscle of Lawrence, a male-specific structure in the abdomen of *Drosophila melanogaster* adults. Development 113:879–890.
Gessa GL, Tagliamonte A (1974) Possible role of brain serotonin and dopamine in controlling male sexual behavior. In: Advances in biochemical psychopharmacology, Vol 11 (Costa E, Gessa GL, Sandler M, eds), pp 217–228. New York: Raven.
Goodwin SF (1999) Molecular neurogenetics of sexual differentiation and behaviour. Curr Opin Neurobiol 9:759–765.
Goodwin SF, Taylor BJ, Villella A, Foss M, Ryner LC, Baker BS, Hall JC (2000) Aberrant splicing and altered spatial expression patterns in *fruitless* mutants of *Drosophila melanogaster*. Genetics 154:725–745.
Greenspan RJ (1995) Understanding the genetic construction of behavior. Sci Am 272(4):72–78.
Hall JC (1978) Courtship among males due to a male-sterile mutation in *Drosophila melanogaster*. Behav Genet 8:125–141.
Hertweck H (1931) Anatomie und Variabilitat des nervensystems und der sinnesorgane von *Drosophila melanogaster* (Meigen). Z Wiss Zool 139:559–663.
Hing A, Carlson JR (1996) Male–male courtship behavior induced by ectopic expression of the *Drosophila white* gene: role of sensory function and age. J Neurobiol 30:327–335.
Ito H, Fujitani K, Usui K, Shimizu-Nishikawa K, Tanaka S, Yamamoto D (1996) Sexual orientation in *Drosophila* is altered by the *satori* mutation in the sex-determination gene *fruitless* that encodes a zinc finger protein with a BTB domain. Proc Natl Acad Sci USA 93:9687–9692.
Lawrence PA, Johnston P (1986) The muscle pattern of a segment of *Drosophila* may be determined by neurons and not by contributing myoblasts. Cell 45:505–513.
Lee G, Foss M, Goodwin SF, Carlo T, Taylor BJ, Hall JC (2000) Spatial, temporal, and sexually dimorphic expression patterns of the *fruitless* gene in the *Drosophila* CNS. J Neurobiol 43:404–426.
Livingstone M, Tempel B (1983) Genetic dissection of monoamine neurotransmitter synthesis in *Drosophila*. Nature 303:67–70.
Miller A (1950) The internal anatomy and histology of the imago of *Drosophila melanogaster*. In: Biology of *Drosophila* (Demerec M, ed), pp 481–495. New York: Wiley.
Monastrioti M (1999) Biogenic amine systems in the fruit fly *Drosophila melanogaster*. Microsc Res Tech 45:106–121.
Nässel DR (1988) Serotonin and serotonin-immunoreactive neurons in the nervous system of insects. Prog Neurobiol 30:1–85.
Nässel DR (1996) Neuropeptides, amines and amino acids in an elementary insect ganglion: functional and chemical anatomy of the unfused abdominal ganglion. Prog Neurobiol 48:325–420.
Nilsson EE, Asztalos Z, Lukacsovich T, Awano W, Usui-Aoki K, Yamamoto D (2000) *fruitless* is in the regulatory pathway by which ectopic *mini-white* and *transformer* induce bisexual courtship in *Drosophila*. J Neurogenet 13:213–232.
Ryner LC, Goodwin SF, Castrillon DH, Anand A, Villella A, Baker BS, Hall JC, Wasserman SA (1996) Control of male sexual behavior and sexual orientation in Drosophila by the *fruitless* gene. Cell 87:1079–1089.
Thorn RS, Truman JW (1994a) Sexual differentiation in the CNS of the moth, *Manduca sexta*. I. Sex and segment-specificity in production, differentiation, and survival of the imaginal midline neurons. J Neurobiol 25:1039–1053.
Thorn RS, Truman JW (1994b) Sexual differentiation in the CNS of the moth, *Manduca sexta*. II. Target dependence for the survival of the imaginal midline neurons. J Neurobiol 25:1054–1066.
Tublitz N, Sylwester AW (1990) Postembryonic alteration of transmitter phenotype in individually identified peptidergic neurons. J Neurosci 10:161–168.
Usui-Aoki K, Ito H, Ui-Yei K, Takahashi J, Lukacsovitch T, Awano W, Nakata H, Piao ZF, Nillson EE, Tomida J, Yamamoto D (2000) Formation of the male-specific muscle in female *Drosophila* by ectopic *fruitless* expression. Nat Cell Biol 2:500–506.
Vallés AM, White K (1986) Development of serotonin-containing neurons in *Drosophila* mutants unable to synthesize serotonin. J Neurosci 6:1482–1491.
Vallés AM, White K (1988) Serotonin-containing neurons in *Drosophila melanogaster*: development and distribution. J Comp Neurol 268:414–428.
Villella A, Hall JC (1996) Courtship anomalies caused by *doublesex* mutations in *Drosophila melanogaster*. Genetics 143:331–334.
Villella A, Gailey DA, Berwald B, Ohshima S, Barnes PT, Hall JC (1997) Extended reproductive roles of the *fruitless* gene in *Drosophila melanogaster* revealed by behavioral analysis of new *fru* mutants. Genetics 147:1107–1130.
Yamamoto D, Nakano Y (1999) Sexual behavior mutants revisited: molecular and cellular basis of *Drosophila* mating. Cell Mol Life Sci 56:634–646.
Zhang S-D, Odenwald WF (1995) Misexpression of the *white* gene triggers male–male courtship in *Drosophila*. Proc Natl Acad Sci USA 92:5525–5529.